Higher-order corrections to Higgs+jet

Frank Petriello

GGI workshop

September 17, 2014

NORTHWESTERN UNIVERSITY

Argonne NATIONAL LABORATORY

Outline

- This talk will focus on improving the modeling of Higgs production in association with jets
  - Resummation of jet-veto logs for the H+jet process
    X. Liu, FP 1210.1906, 1303.4405; R, Boughezal, X. Liu, FP, F. Tackmann, J. Walsh 1312.4535
  - NNLO fixed-order predictions for Higgs+jet
    R. Boughezal, F. Caola, K. Melnikov, FP, M. Schulze 1302.6216

The Higgs circa 2014

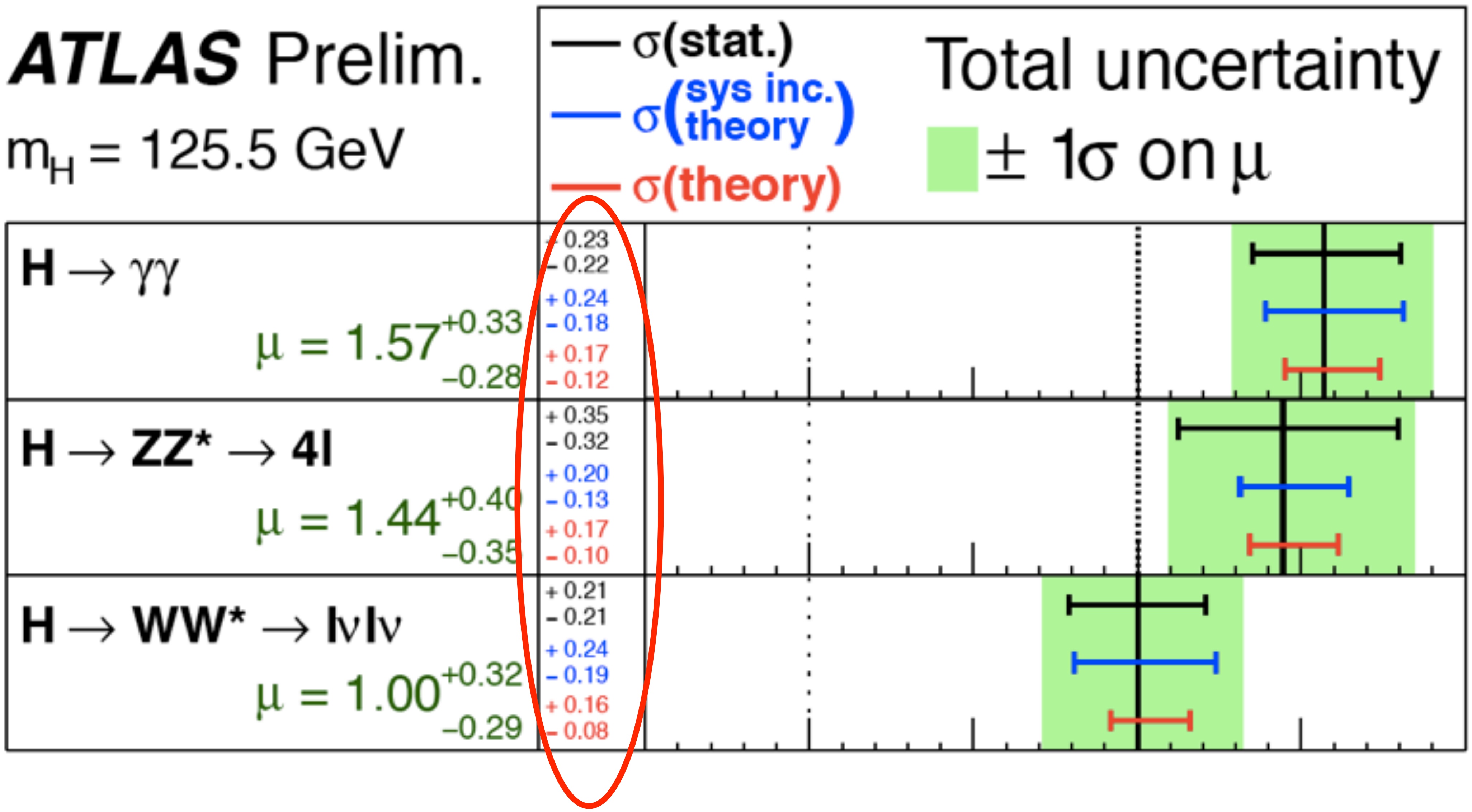

- The dominant component of the systematic error is theory
- Will become a limiting factor in interpretation in Run II as statistical errors decrease

A two-front war

- Two reasons for the dominance of theory uncertainties in Higgs analyses

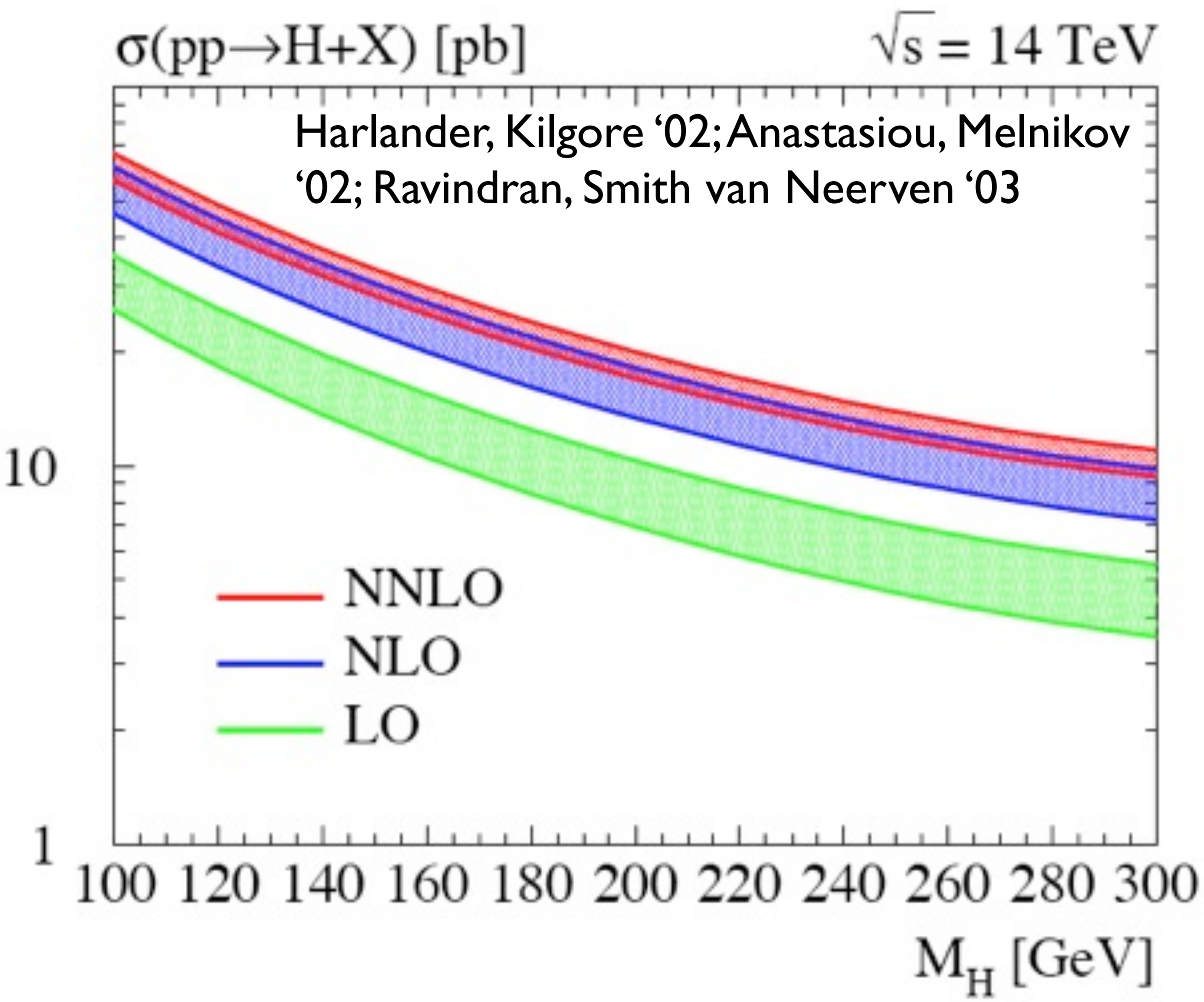

Large fixed-order QCD corrections to Higgs production processes

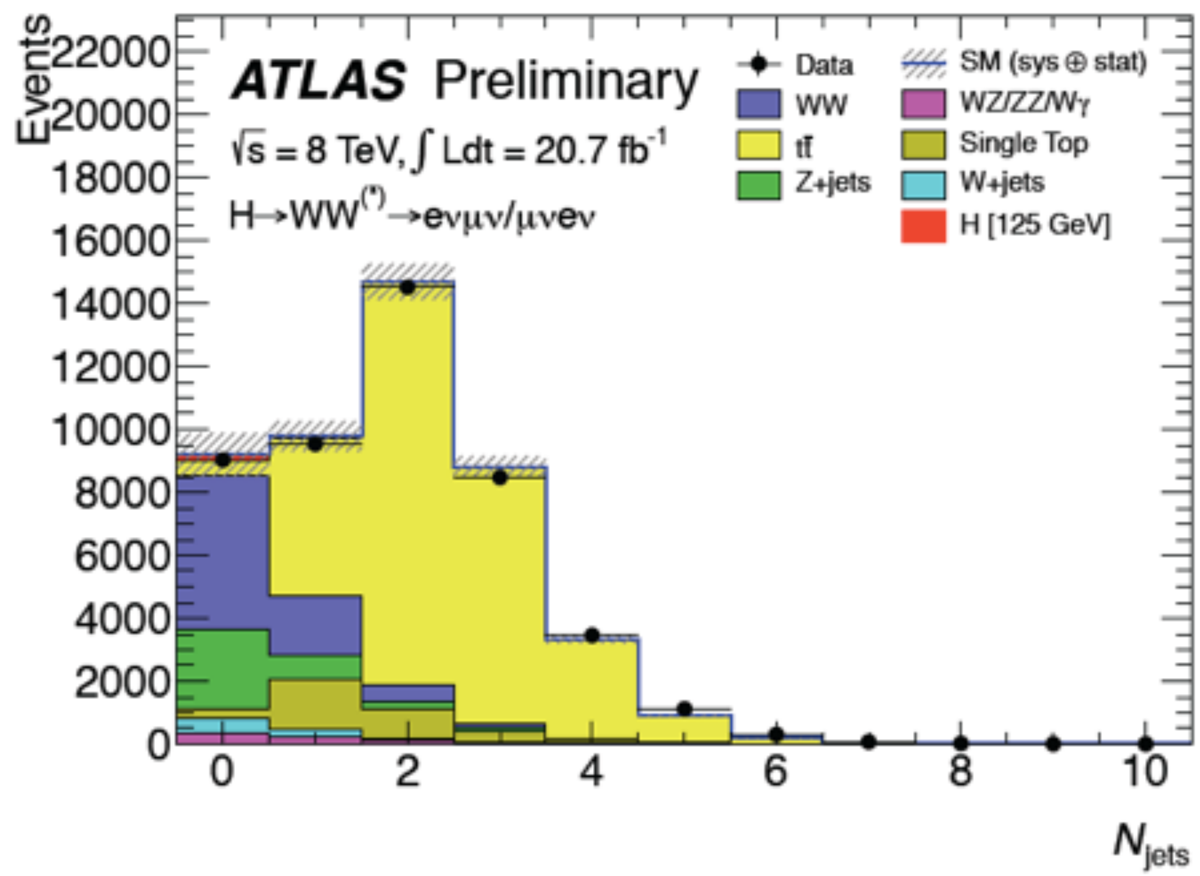

Division into exclusive jet bins introduces large logarithms that must be resummed

- Progress on both fronts needed to improve Higgs-signal modeling for Run II of the LHC

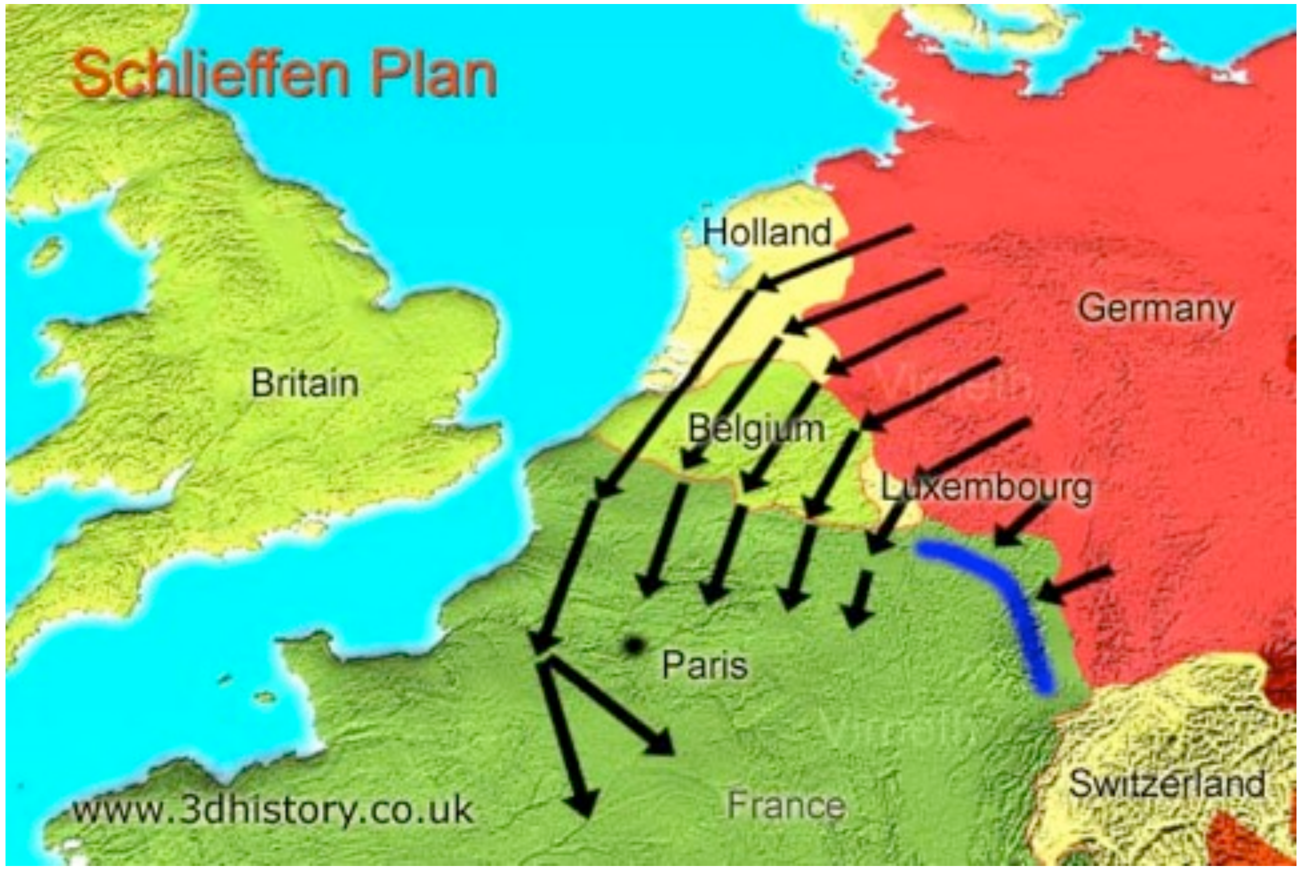

Resummation of jet-veto logarithms in the exclusive 1-jet bin

Exclusive jet binning

- A major issue in the WW channel is the division into exclusive jet bins

Source ATLAS	$N_{jet} = 0$	$N_{jet} = 1$	$N_{jet} \geq 2$
Theoretical uncertainties on total signal yield (%)			
QCD scale for ggF, $N_{jet} \geq 0$	+13	-	-
QCD scale for ggF, $N_{jet} \geq 1$	+10	−27	-
QCD scale for ggF, $N_{jet} \geq 2$	-	−15	+4
QCD scale for ggF, $N_{jet} \geq 3$	-	-	+4
Parton shower and underlying event	+3	−10	±5
QCD scale (acceptance)	+4	+4	±3
Experimental uncertainties on total signal yield (%)			
Jet energy scale and resolution	5	2	6
Uncertainties on total background yield (%)			
WW transfer factors (theory)	±1	±2	±4
Jet energy scale and resolution	2	3	7
b-tagging efficiency	-	+7	+2
f_{recoil} efficiency	±4	±2	-

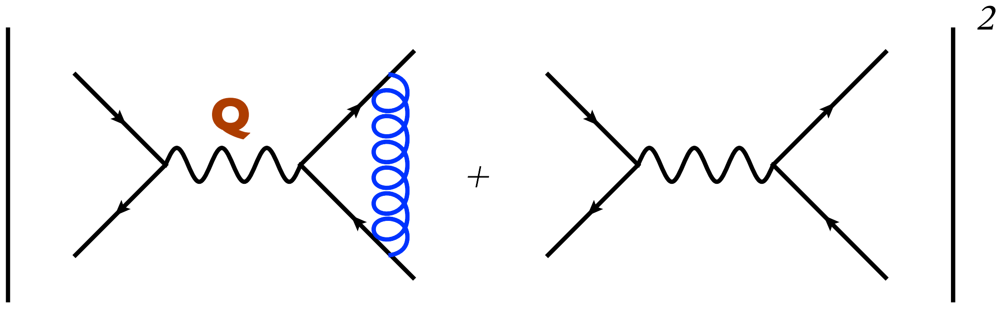

Virtual corrections: $-1/\varepsilon_{IR}^2$

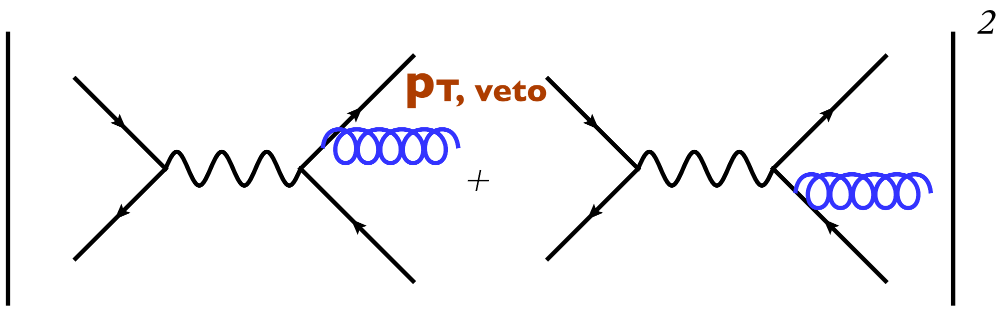

Real corrections: $1/\varepsilon_{IR}^2 - a\times\ln^2(Q/p_{T,veto})$

- Relevant term for gluon-fusion Higgs searches: $2C_A(\alpha_S/\pi)\ln^2(M_H/p_{T,veto}) \sim 1/2 \Rightarrow$ potentially a large correction

Effects of the jet veto

Stewart, Tackmann 1107.2117

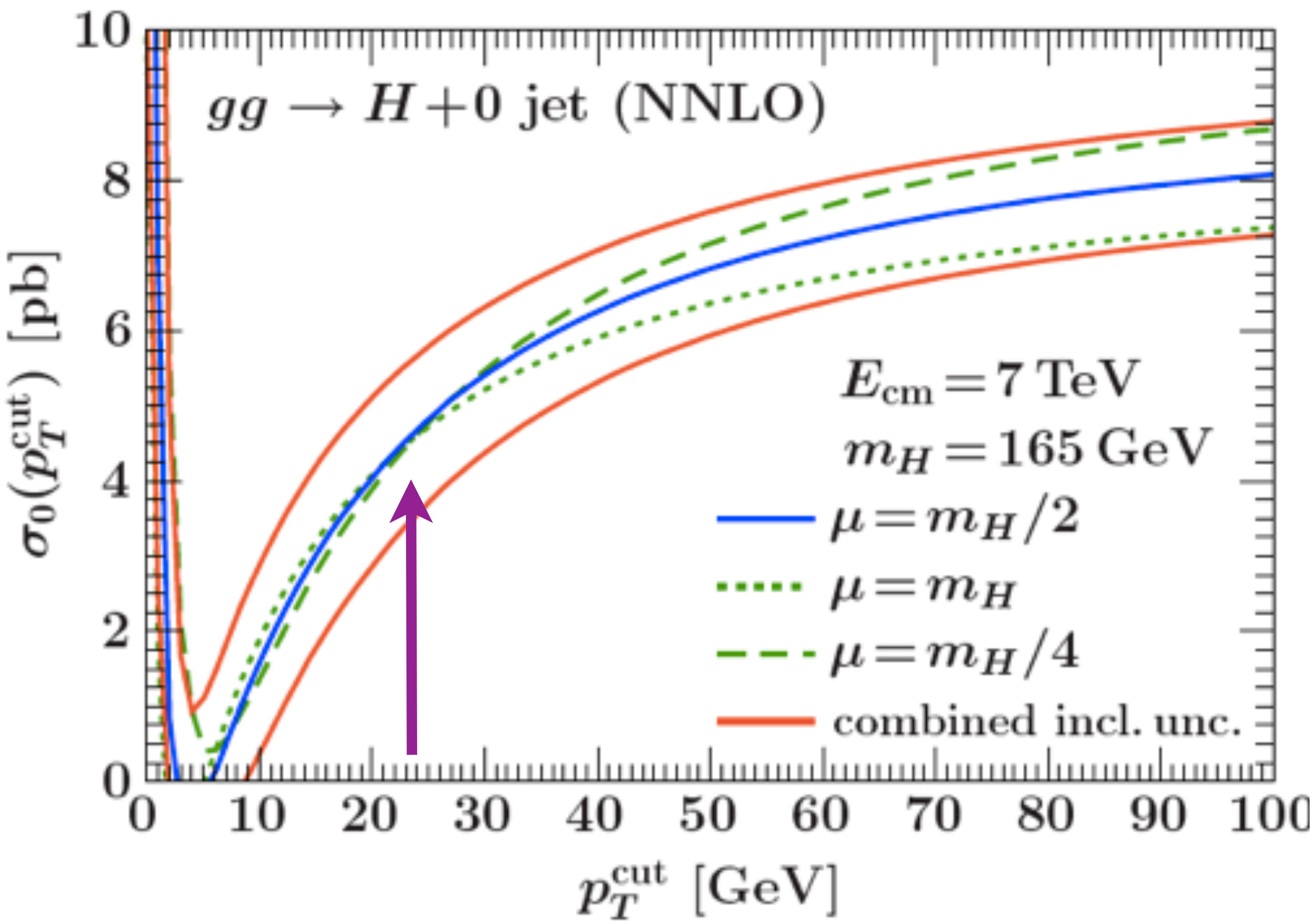

X. Liu, FP 1303.4405

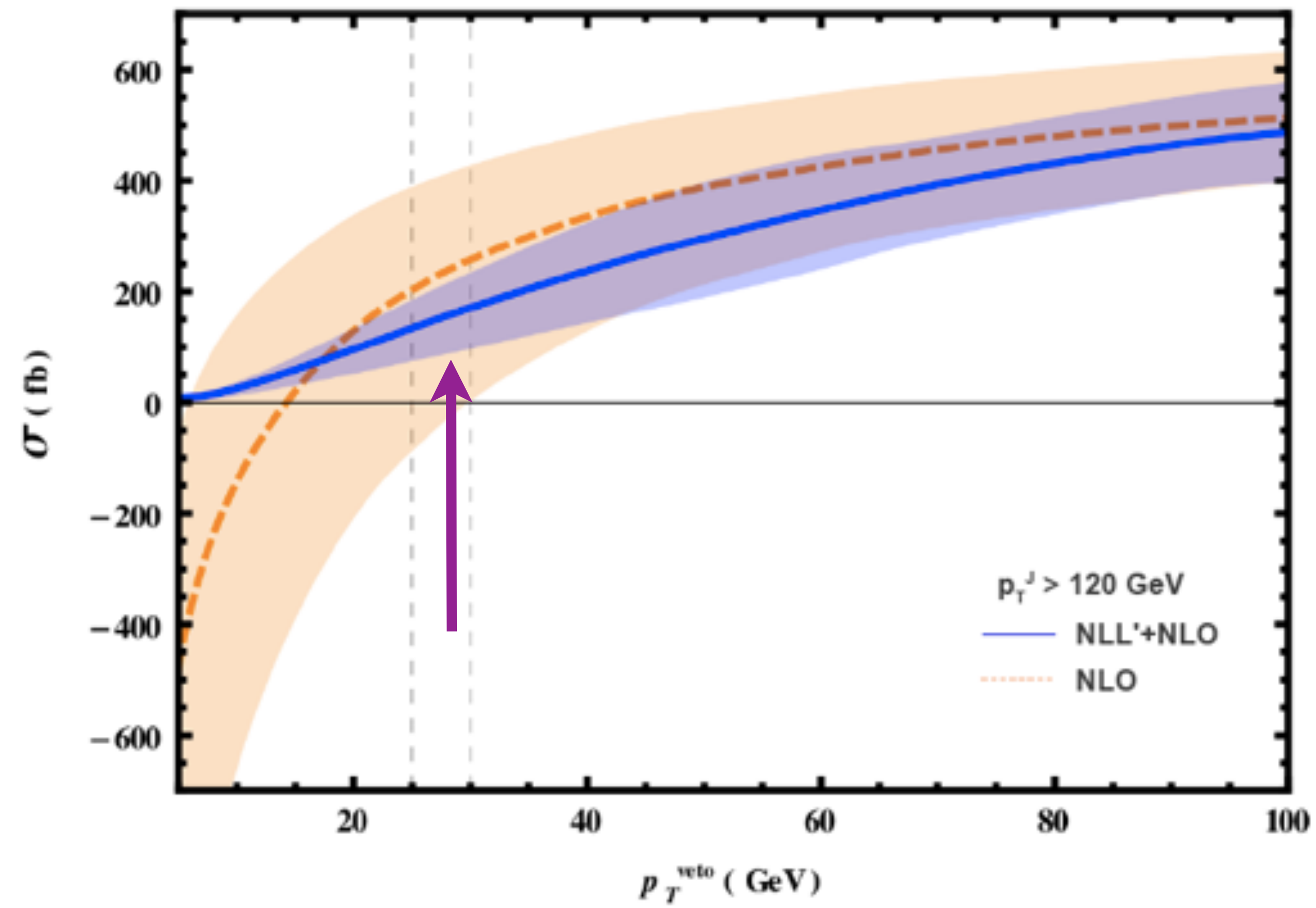

- Breakdown of the usual scale-variation method for estimating theory uncertainties

- Deviations from fixed-order perturbation theory, especially in new kinematic regions that will be first probed in Run II

Current error treatment

- Current covariance matrix used by ATLAS and CMS follows the Stewart-Tackmann (ST) prescription:

$$C_{\mathrm{FO}}(\{\sigma_0,\sigma_1,\sigma_{\geq 2}\}) = \begin{pmatrix} (\Delta^{\mathrm{FO}}_{\geq 0})^2 + (\Delta^{\mathrm{FO}}_{\geq 1})^2 & -(\Delta^{\mathrm{FO}}_{\geq 1})^2 & 0 \\ -(\Delta^{\mathrm{FO}}_{\geq 1})^2 & (\Delta^{\mathrm{FO}}_{\geq 1})^2 + (\Delta^{\mathrm{FO}}_{\geq 2})^2 & -(\Delta^{\mathrm{FO}}_{\geq 2})^2 \\ 0 & -(\Delta^{\mathrm{FO}}_{\geq 2})^2 & (\Delta^{\mathrm{FO}}_{\geq 2})^2 \end{pmatrix}$$

$\Delta_{\geq 0}$: fixed-order uncertainty on total cross section (NNLO)

$\Delta_{\geq 1}$: fixed-order uncertainty on inclusive 1-jet rate (NLO)

$\Delta_{\geq 2}$: fixed-order uncertainty on inclusive 2-jet rate (LO/NLO)

- The logic: the perturbative series for the inclusive cross sections are independent in the small p_T^{cut} limit, so add in quadrature. By construction, the 0-jet and 1-jet exclusive uncertainties are greater than the inclusive 0-jet and 1-jet uncertainties

Current error treatment

- Current covariance matrix used by ATLAS and CMS follows the Stewart-Tackmann (ST) prescription:

$$C_{\rm FO}(\{\sigma_0,\sigma_1,\sigma_{\geq 2}\}) = \begin{pmatrix} (\Delta^{\rm FO}_{\geq 0})^2 + (\Delta^{\rm FO}_{\geq 1})^2 & -(\Delta^{\rm FO}_{\geq 1})^2 & 0 \\ -(\Delta^{\rm FO}_{\geq 1})^2 & (\Delta^{\rm FO}_{\geq 1})^2 + (\Delta^{\rm FO}_{\geq 2})^2 & -(\Delta^{\rm FO}_{\geq 2})^2 \\ 0 & -(\Delta^{\rm FO}_{\geq 2})^2 & (\Delta^{\rm FO}_{\geq 2})^2 \end{pmatrix}$$

$\Delta_{\geq 0}$: fixed-order uncertainty on total cross section (NNLO)

$\Delta_{\geq 1}$: fixed-order uncertainty on inclusive 1-jet rate (NLO)

$\Delta_{\geq 2}$: fixed-order uncertainty on inclusive 2-jet rate (LO/NLO)

- The goal: completely replace fixed-order perturbation theory with renormalization-group improved PT that resums the large jet-veto logs. We will see that there is a significant numerical improvement resulting from this replacement.

Zero-jet resummation

- Begin in the zero-jet bin. Current status with anti-k_T algorithm:
  - Banfi, Monni, Salam, Zanderighi: NNLL'+NNLO 1203.5573, 1206.4998, 1308.4634
  - Becher, Neubert NNLL+NNLO 1205.3806, partial N^{3}LL+NNLO 1307.0025
  - Stewart, Tackmann, Walsh, Zuberi NNLL'+NNLO 1307.1808

Counting in the log of the cross section

LL	NLL	NLL$'$ / NNLL	NNLL$'$ / NNNLL	
$\alpha_s L^2$	$\alpha_s L$	α_s		
$\alpha_s^2 L^3$	$\alpha_s^2 L^2$	$\alpha_s^2 L$	α_s^2	
$\alpha_s^3 L^4$	$\alpha_s^3 L^3$	$\alpha_s^3 L^2$	$\alpha_s^3 L$	α_s^3

$$L = \ln \frac{p_T^{\mathrm{cut}}}{m_H}$$

Global veto log structure

NNLL’+NNLO resummation

green: NLL_{p_T}
blue: NLL'_{p_T} +NLO
orange: NNLL'_{p_T} +NNLO

- Significant improvement in prediction from including higher-order resummation and fixed-order

Including resummation and fixed-order uncertainties

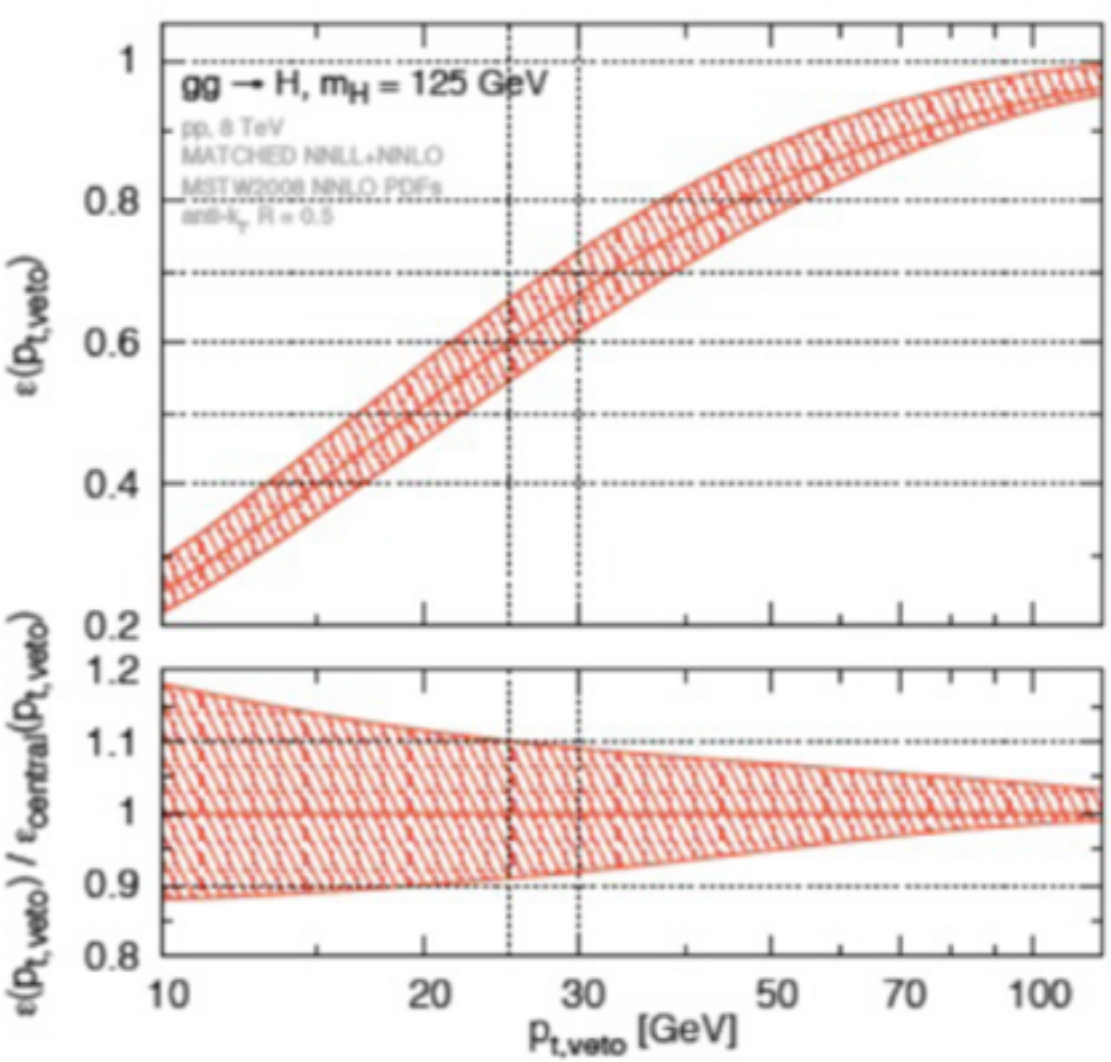

Banfi, Monni, Salam, Zanderighi 1206.4998

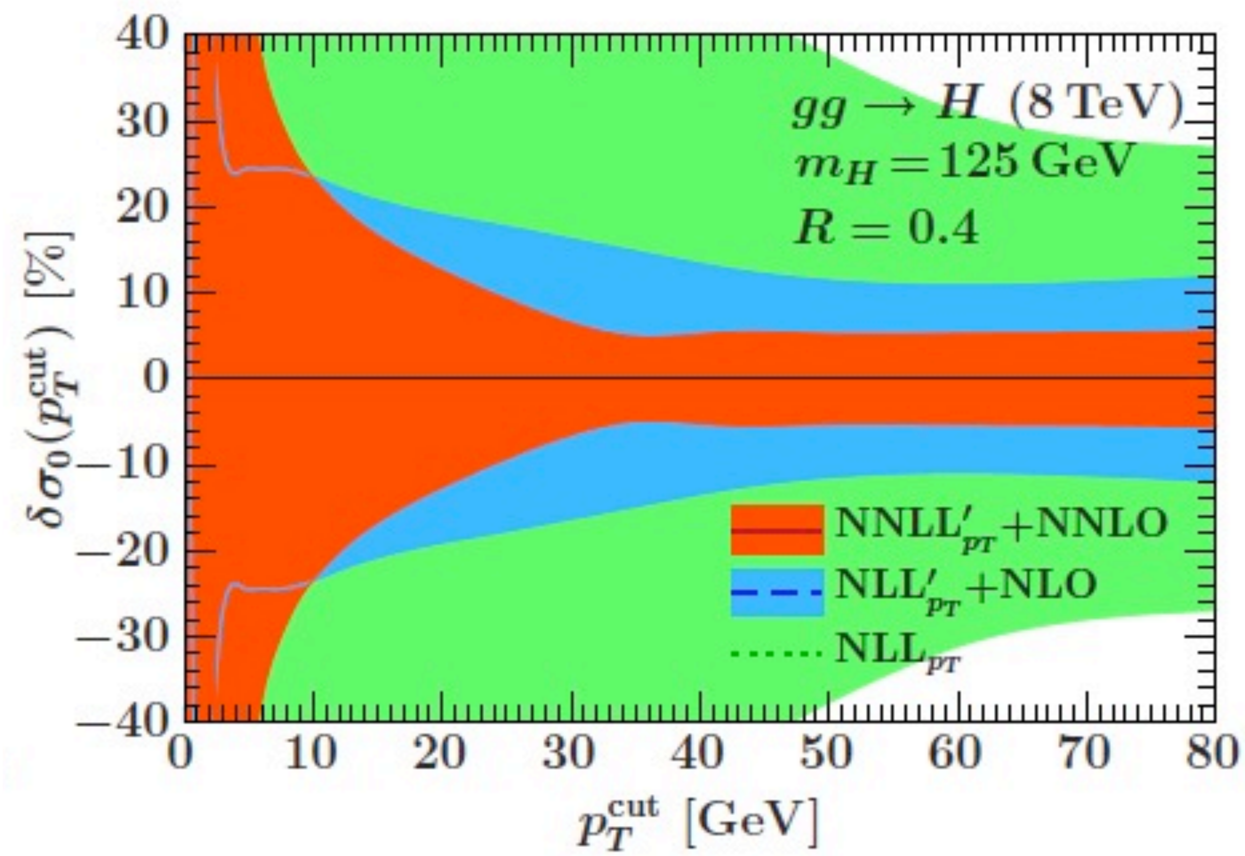

Stewart, Tackmann, Walsh, Zuberi 1307.1808

The one-jet bin: high-p_T

- Now discuss the jet-veto logarithms in the H+1 jet bin
- Two relevant regions of jet p_T: $p_T \sim m_H >> p_{T,veto}$, $m_H >> p_T \sim p_{T,veto}$
- Currently can directly resum at NLL'+NLO the first region

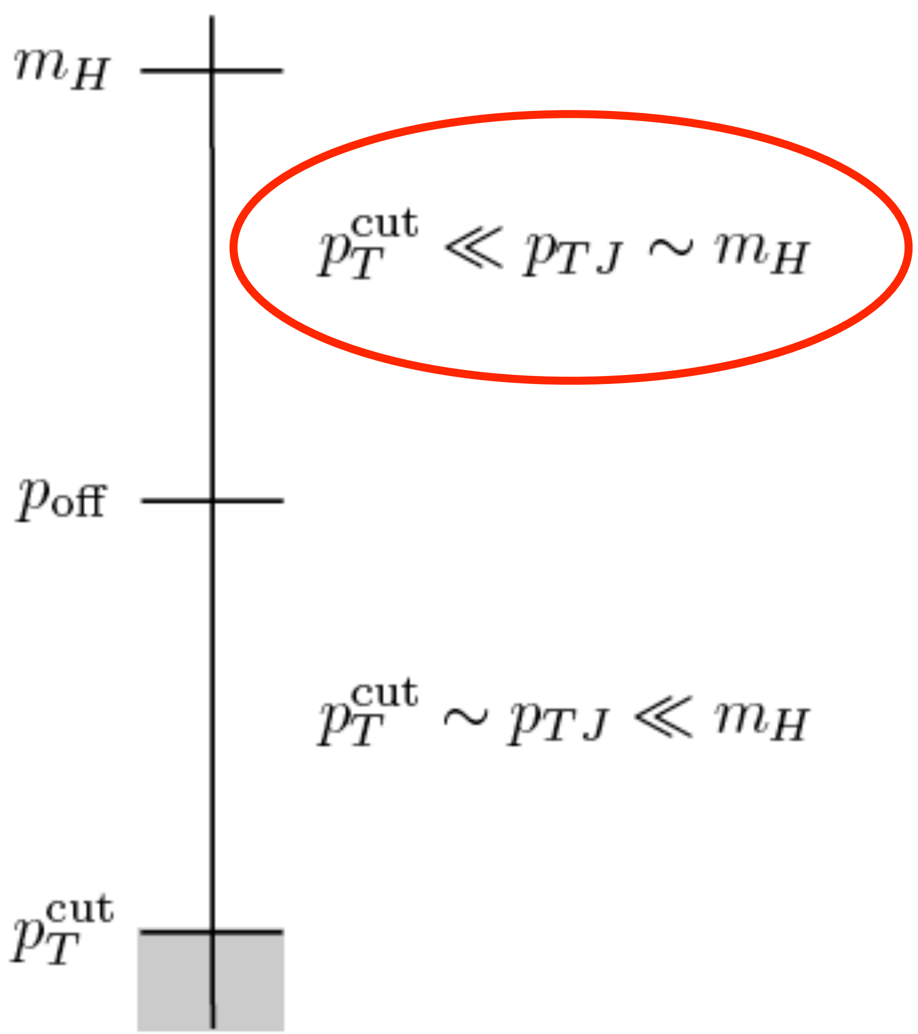

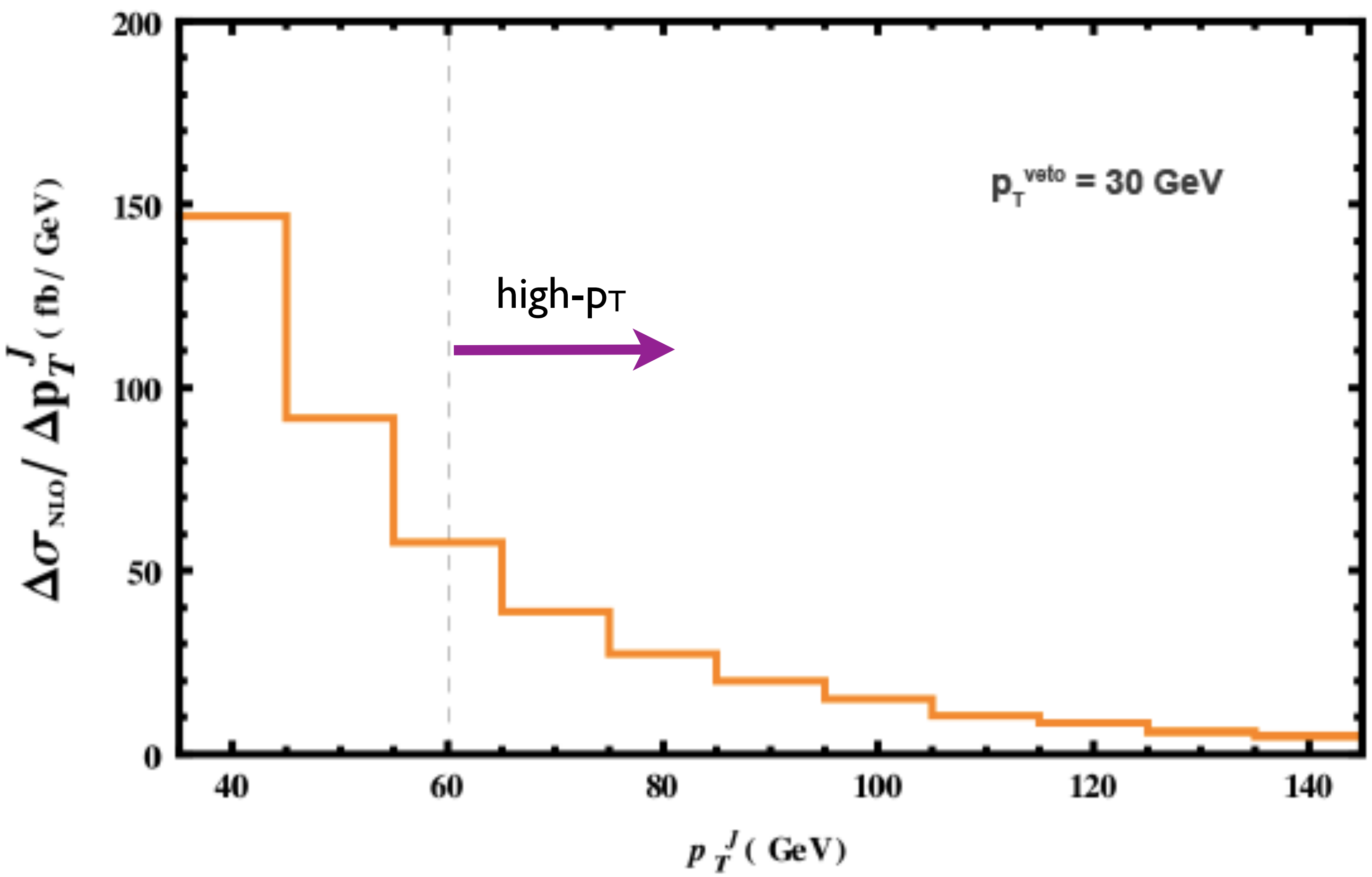

- Comprises roughly 30% of the event rate at the 8 TeV LHC...

The one-jet bin: high-p_T

- Now discuss the jet-veto logarithms in the H+1 jet bin
- Two relevant regions of jet p_T: $p_T \sim m_H >> p_{T,veto}$, $m_H >> p_T \sim p_{T,veto}$
- Currently can directly resum at NLL'+NLO the first region

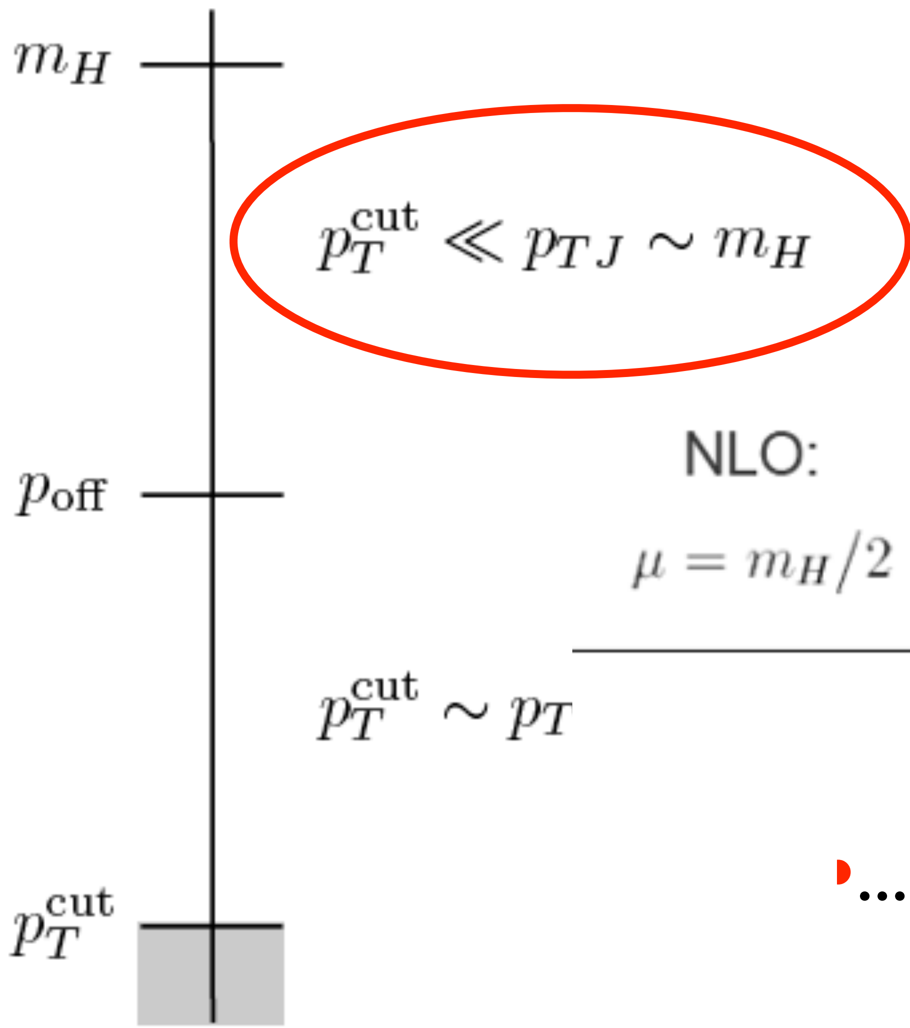

NLO:	$\sigma(p_T^J > 30)(\mathrm{pb})$	$\sigma(63 > p_T^J > 30)(\mathrm{pb})$	$\sigma(p_T^J > 63)(\mathrm{pb})$
$\mu = m_H/2$	$5.2^{+1.65}_{-2.12}$	$3.9^{+1.01}_{-0.95}$	$1.3^{+0.75}_{-1.30}$

- ... but makes up roughly 50% of the 1-jet bin error

The EFT

- We utilize an EFT approach:

$p_s \sim m_H(\lambda,\lambda,\lambda)$

$p_{a,b} \sim m_H(\lambda^2,1,\lambda)$ $\qquad \lambda \equiv p_T^{veto}/\sqrt{\hat{s}} \ll 1$

$p_J \sim m_H(\lambda^2,1,\lambda)$ (along jet direction)

- Distance measures for H+1 jet, anti-k_T algortihm:

$$\rho_{ij} = \min(p_{T,i}^{-1}, p_{T,j}^{-1})\Delta R_{ij}/R,$$
$$\rho_i = p_{T,i}^{-1}.$$

$$\rho_{JJ} \lesssim \rho_J \sim 1\,, \quad \rho_{Js} \sim R^{-1}\,, \quad \rho_{Ja} \sim \rho_{Jb} \sim R^{-1}\log\lambda^{-1}\,,$$
$$\rho_{ss} \sim \rho_{aa} \sim \rho_{bb} \sim (\lambda R)^{-1}\,, \quad \rho_{sa} \sim \rho_{sb} \sim \rho_{ab} \sim (\lambda R)^{-1}\log\lambda^{-1}\,,$$
$$\rho_s \sim \rho_a \sim \rho_b \sim \lambda^{-1}\,.$$

R~0.4, λ~0.2

- Radiation along the jet direction is combined first into a single state; soft radiation insensitive to details of collinear radiation

Factorization theorem

- Establish the following result for the NLL' resummed cross section

$$
\begin{aligned}
\mathrm{d}\sigma_{\mathrm{NLL'}} &= \mathrm{d}\Phi_H \mathrm{d}\Phi_J\, \mathcal{F}(\Phi_H, \Phi_J) \sum_{a,b} \int \mathrm{d}x_a \mathrm{d}x_b \frac{1}{2\hat{s}} (2\pi)^4 \delta^4 (q_a + q_b - q_J - q_H) \\
&\times \overline{\sum_{\text{spin}}}\, \overline{\sum_{\text{color}}} \operatorname{Tr}(H \cdot S)\, \mathcal{I}_{a, i_a j_a} \otimes f_{j_a}(x_a)\, \mathcal{I}_{b, i_b j_b} \otimes f_{j_b}(x_b)\, J_J(R)\,.
\end{aligned}
$$

virtual corrections　soft radiation　beam-collinear radiation　jet-collinear radiation

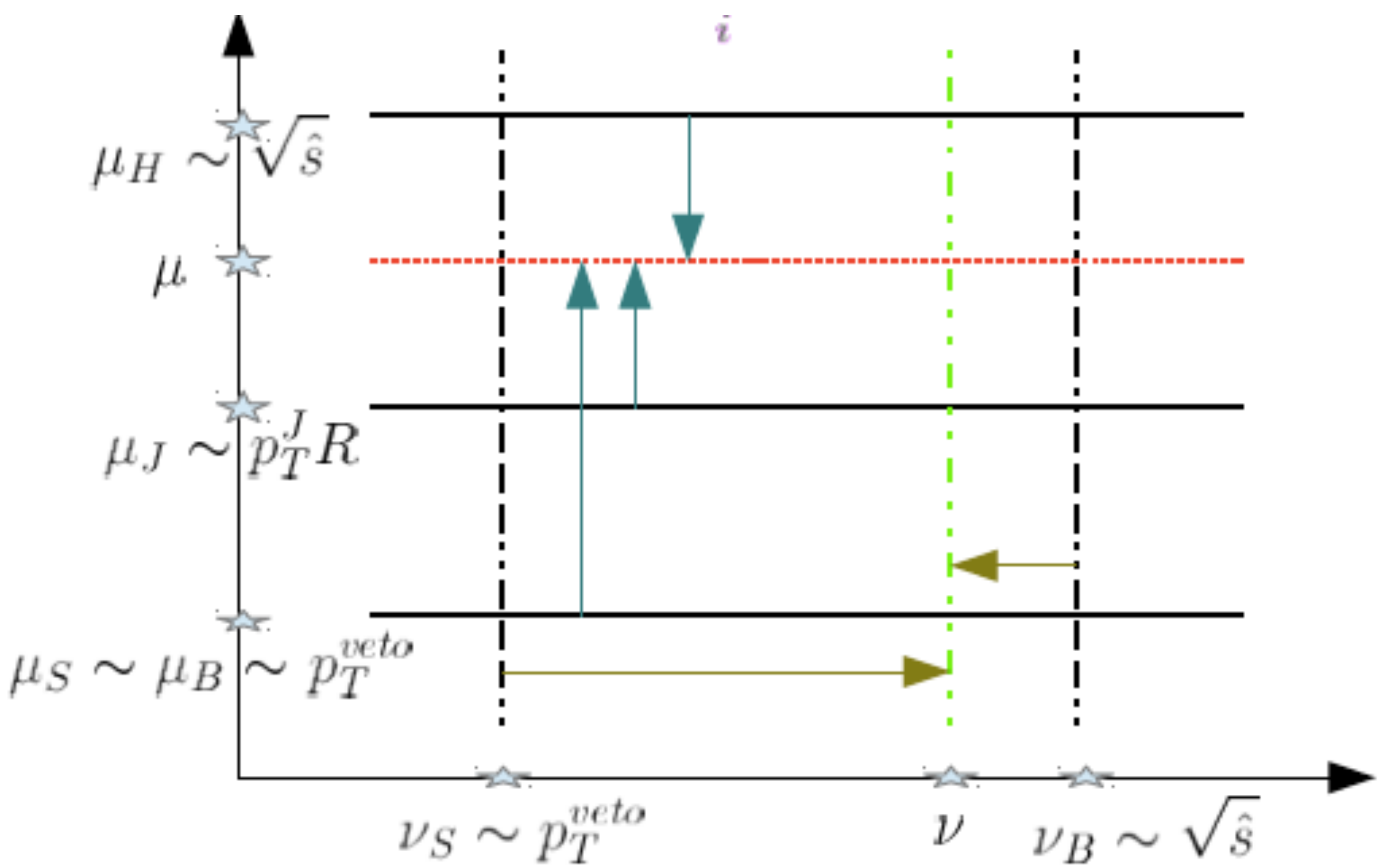

- Resummation of large logs accomplished through RG evolution of each function from its natural scale to a common scale μ

Non-global logarithms

•Non-global logs: correlated emissions from inside the jet-cone to outside.
Dasgupta, Salam hep-ph/0104277

•Not captured in the factorization formula presented

•Large N_C resummation of these terms for an energy veto indicates that they are numerically irrelevant (<1%), but it would be nice to understand their structure better

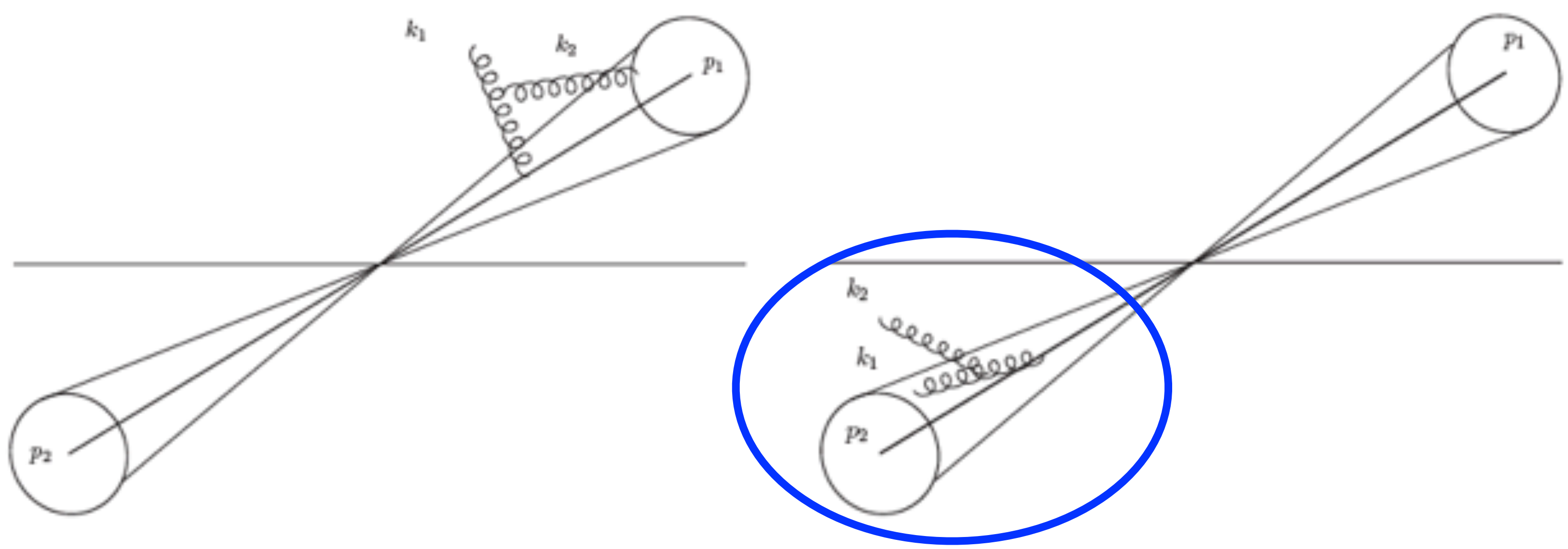

Figure 1: Diagrams representing the correlated emissions which give rise to the lowest-order non-global logarithms. On the left: the harder gluon k_1 lies outside both jets and the softest one k_2 is recombined with the measured jet and contributes to the jet-mass distribution. On the right: the harder gluon is inside the unmeasured jet and emits a softer gluon outside both jets, which contributes to the E_0-distribution.

Numerical results

- Integrate over entire p_T range used in the ATLAS measurement

X. Liu, FP 1303.4405

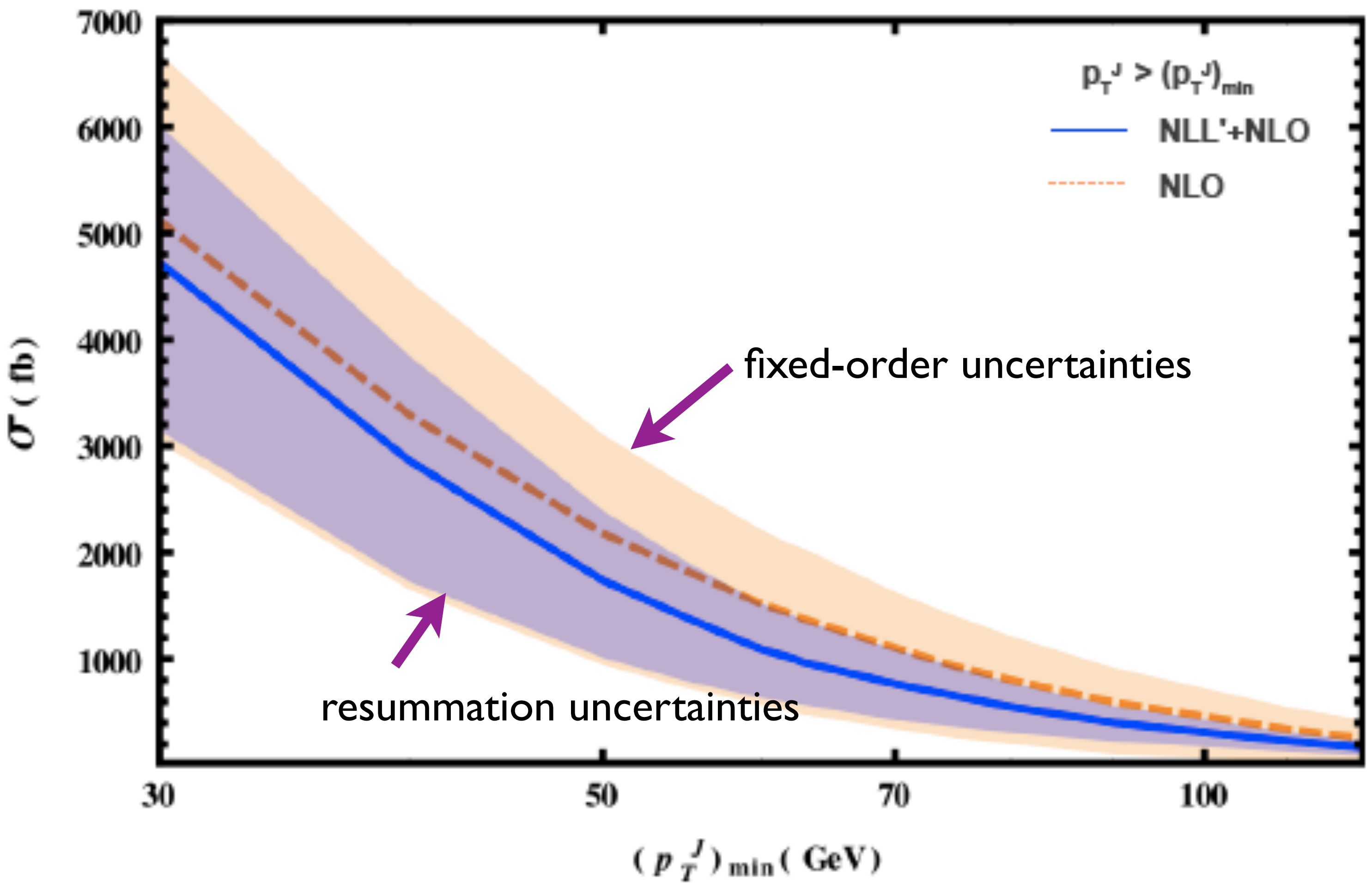

- Resummation uncertainties: separately vary all scale (hard, jet, beam+soft, non-singular) around their central values, add in quadrature

- Large uncertainty from the high-p_T region makes this resummation very effective in reducing errors
- Very conservatively (turn off resummation at $p_{T,J}=m_H/2$, use ST below this value) error on the entire1-jet bin result is decreased by 25%
- But we can do better...

The one-jet bin: low-p_T

- We can indirectly sum the low-p_T one-jet region in the following way
- Cross section of interest: $\sigma_1(p_{off}, p_{Tcut}; p_{Tcut})$

Leading-jet: $p_{Tcut} < p_{T1} < p_{off}$

Veto on second jet

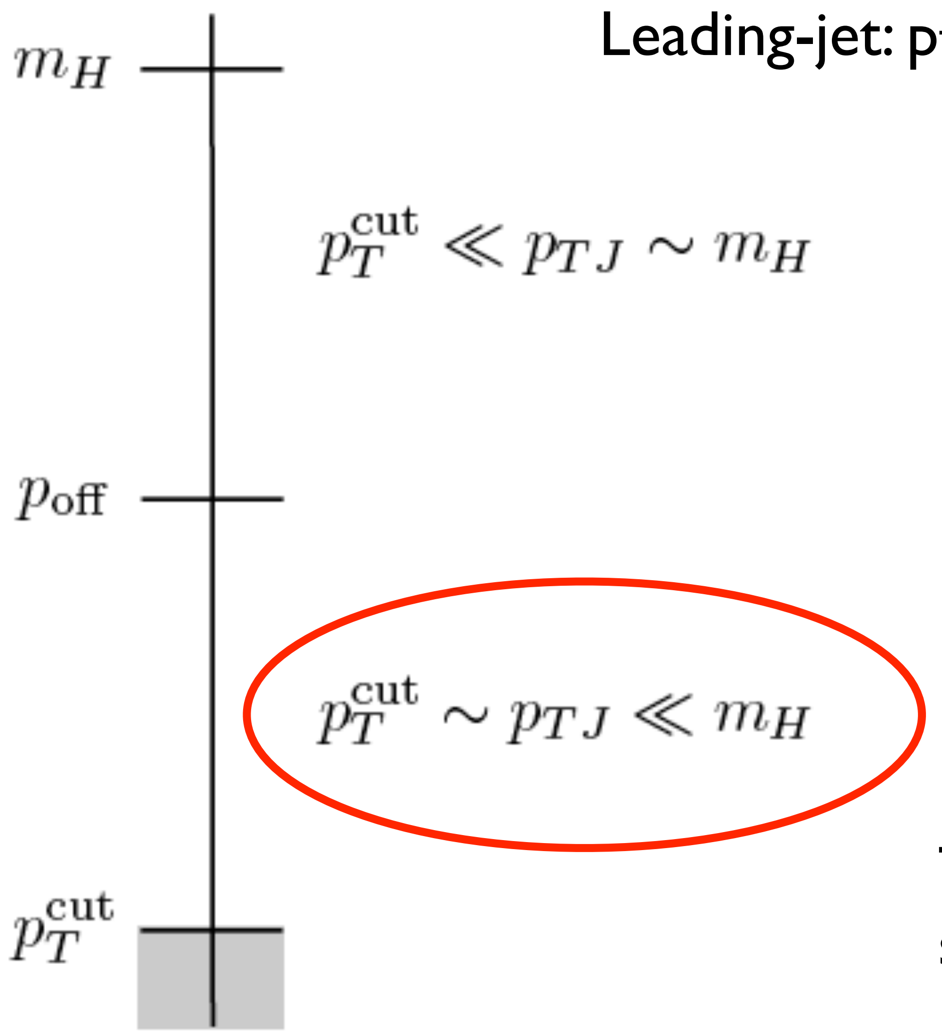

Difference of 0-jet cross sections with p_T less than the indicated argument

$$\sigma_1(p_{off}, p_{Tcut}; p_{Tcut}) = \sigma_0(p_{off}) - \sigma_0(p_{Tcut})$$

$$- \sigma_{\geq 2}(p_{Tcut}) + \sigma_{\geq 2}(p_{off}, p_{Tcut})$$

Two-jet inclusive cross section with $p_{T1}, p_{T2} > p_{Tcut}$

Two-jet inclusive cross section with $p_{T1} > p_{off}, p_{T2} > p_{Tcut}$

The one-jet bin: low-p_T

- We can indirectly sum the low-p_T one-jet region in the following way
- Cross section of interest: $\sigma_1(p_{off}, p_{Tcut}; p_{Tcut})$

Leading-jet: $p_{Tcut} < p_{T1} < p_{off}$ Veto on second jet

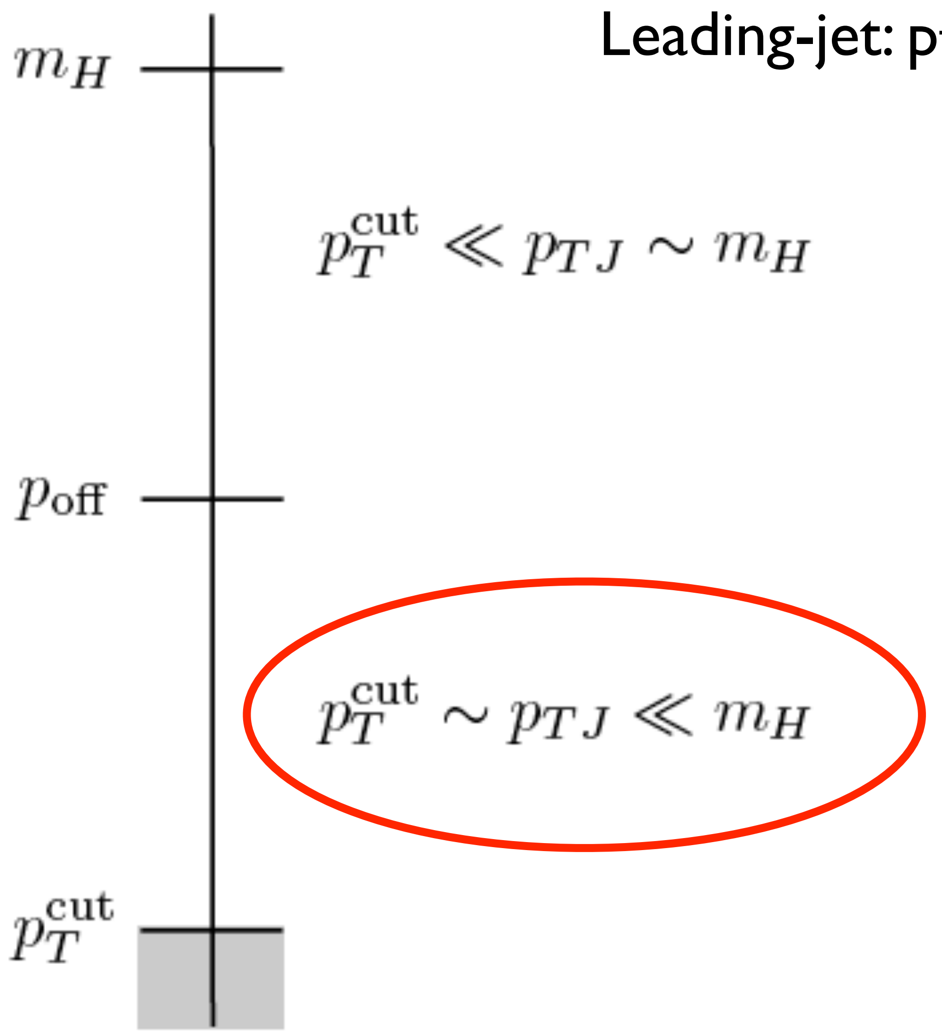

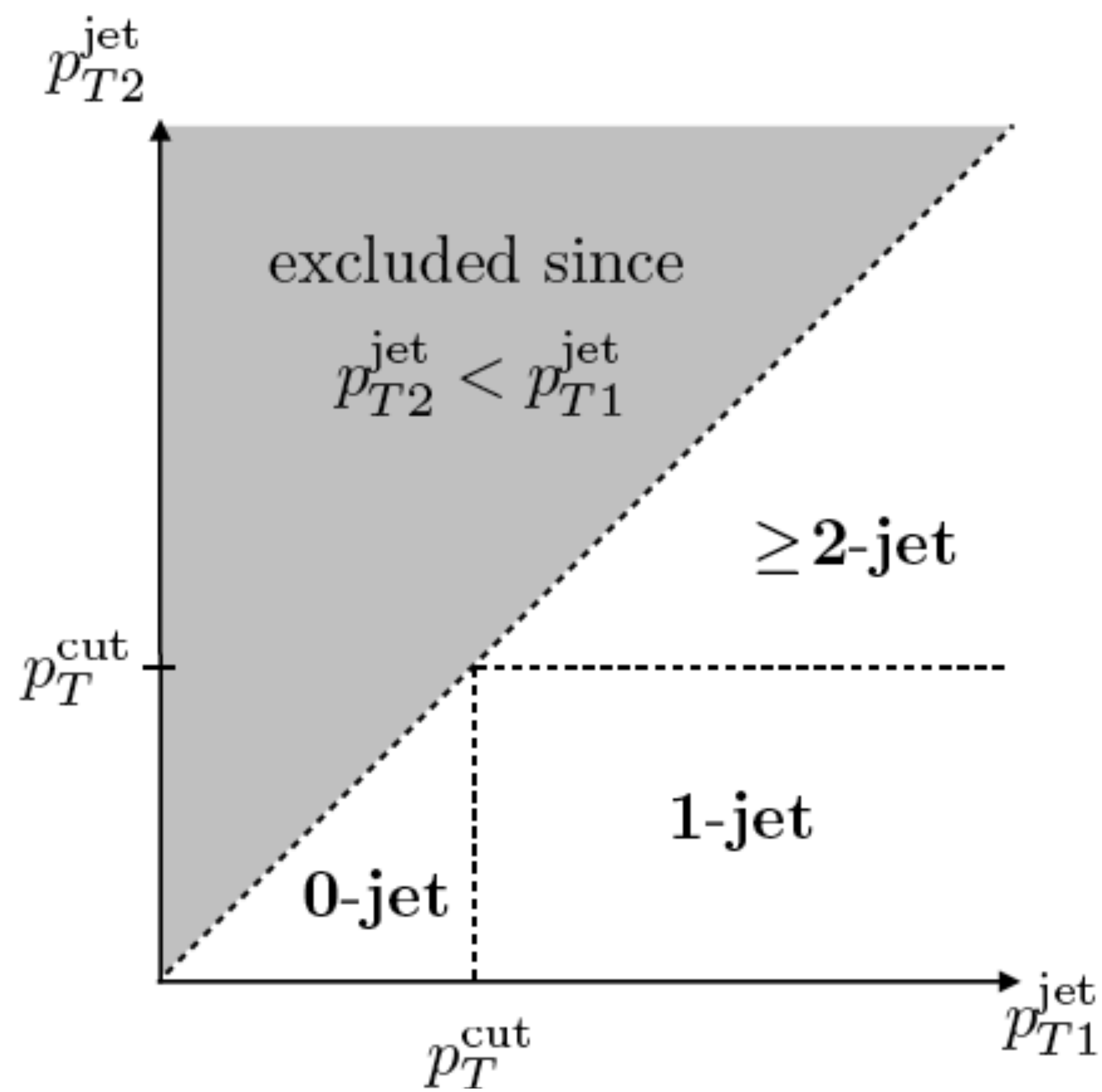

The one-jet bin: low-p_T

- We can indirectly sum the low-p_T one-jet region in the following way
- Cross section of interest: $\sigma_1(p_{off}, p_{Tcut}; p_{Tcut})$

Leading-jet: $p_{Tcut} < p_{T1} < p_{off}$

Veto on second jet

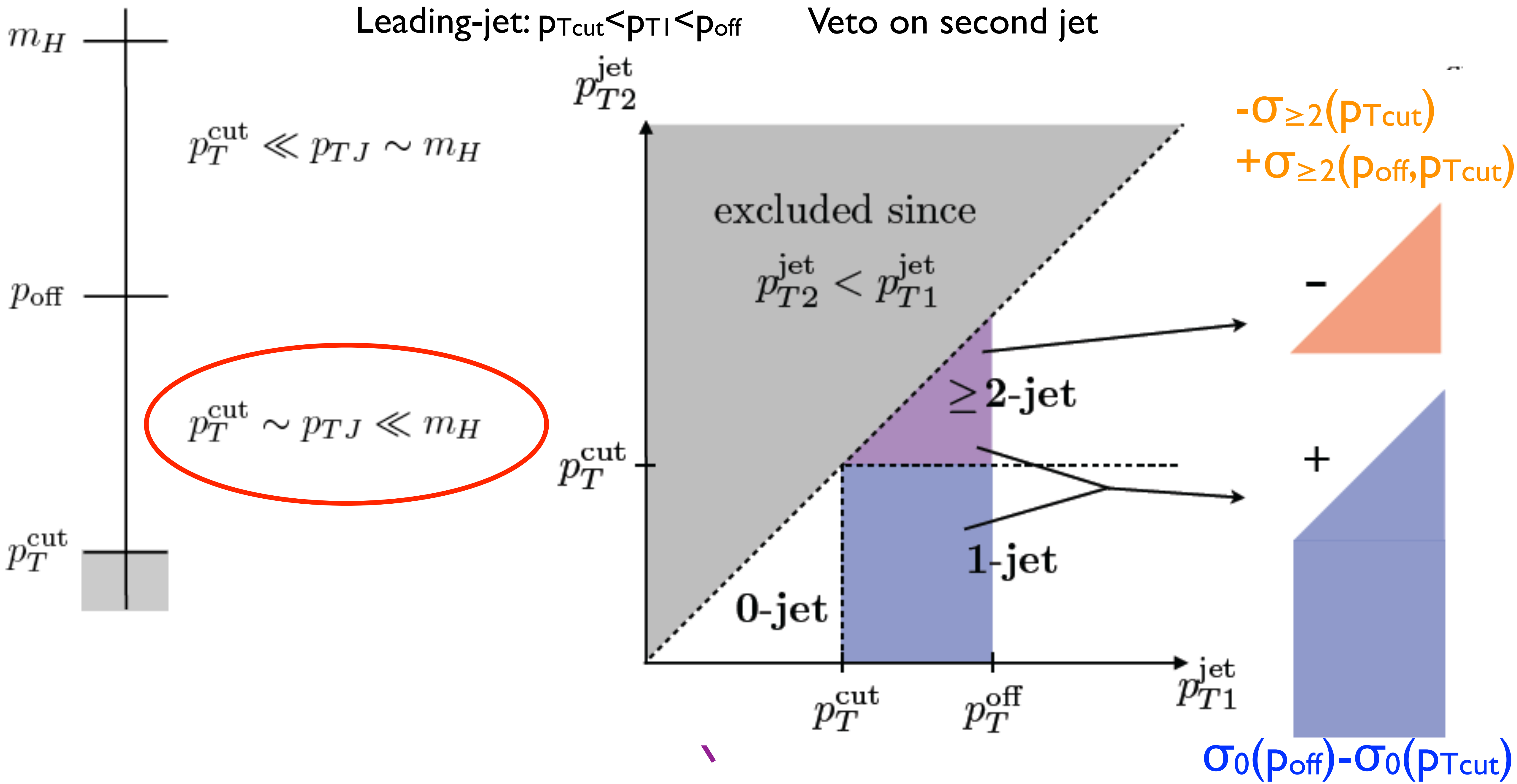

The one-jet bin: low-p_T

- We can indirectly sum the low-p_T one-jet region in the following way
- Cross section of interest: $\sigma_1(p_{off}, p_{Tcut}; p_{Tcut})$

Leading-jet: $p_{Tcut} < p_{T1} < p_{off}$ Veto on second jet

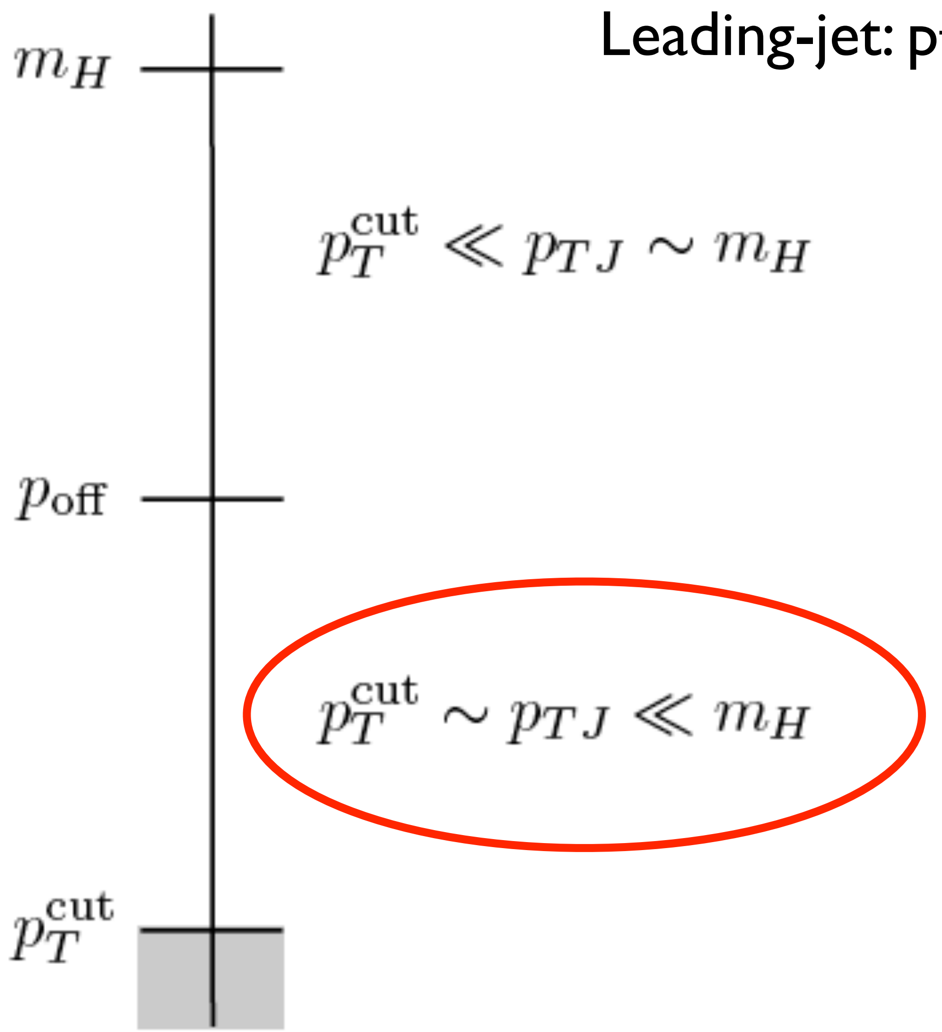

$$\sigma_1(p_{off}, p_{Tcut}; p_{Tcut}) = \sigma_0(p_{off}) - \sigma_0(p_{Tcut})$$
$$- \sigma_{\geq 2}(p_{Tcut}) + \sigma_{\geq 2}(p_{off}, p_{Tcut})$$

- This is an identity if both side are computed to the same order in α_s
- We can resum the jet-veto logs in the 0-jet terms, but not the 2-jet ones
- If $\Delta\sigma_0 \gg \Delta\sigma_{\geq 2}$, we can RG-improve the 0-jet terms on the RHS, and this constitutes an improvement of the low-p_T 1-jet bin

The one-jet bin: low-p_T

- We can indirectly sum the low-p_T one-jet region in the following way
- Cross section of interest: $\sigma_1(p_{off}, p_{Tcut}; p_{Tcut})$

$$\sigma_1(p_{off}, p_{Tcut}; p_{Tcut}) = \sigma_0(p_{off}) - \sigma_0(p_{Tcut})$$
$$- \sigma_{\geq 2}(p_{Tcut}) + \sigma_{\geq 2}(p_{off}, p_{Tcut})$$

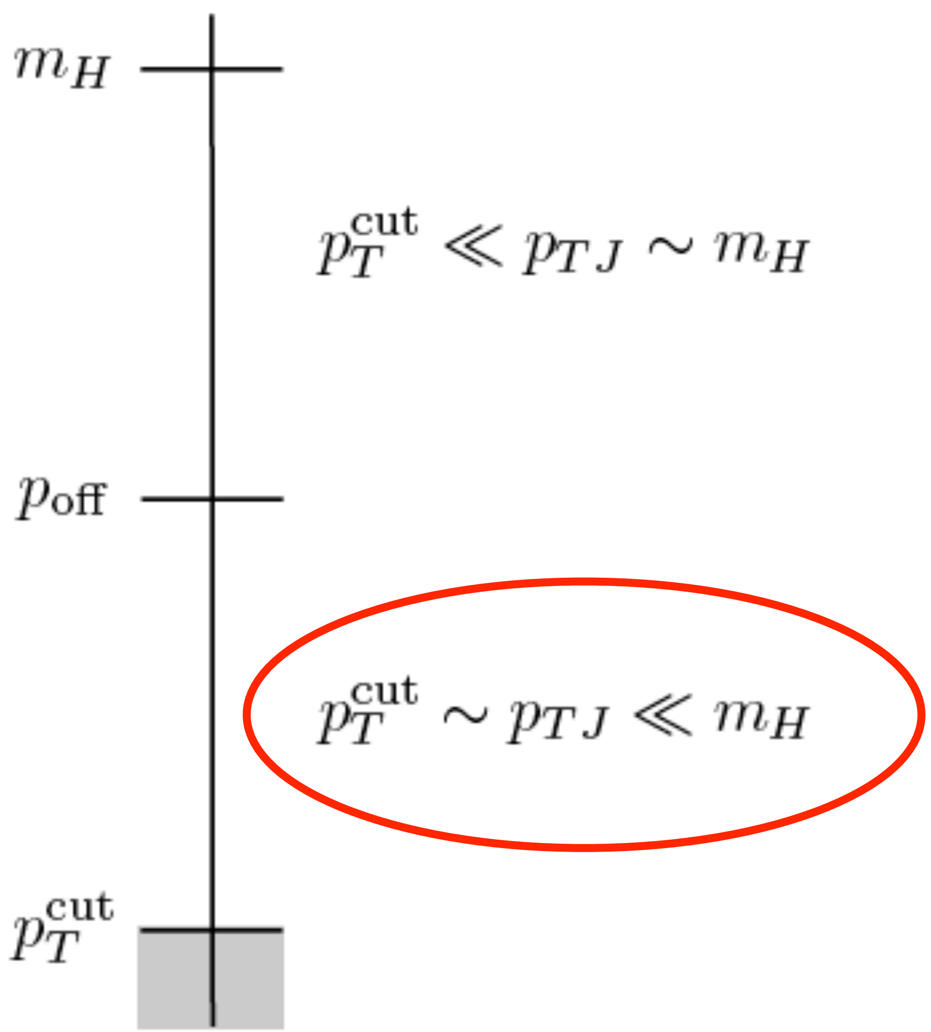

- The two-jet pieces are a small fraction of the one-jet rate, 10% or less

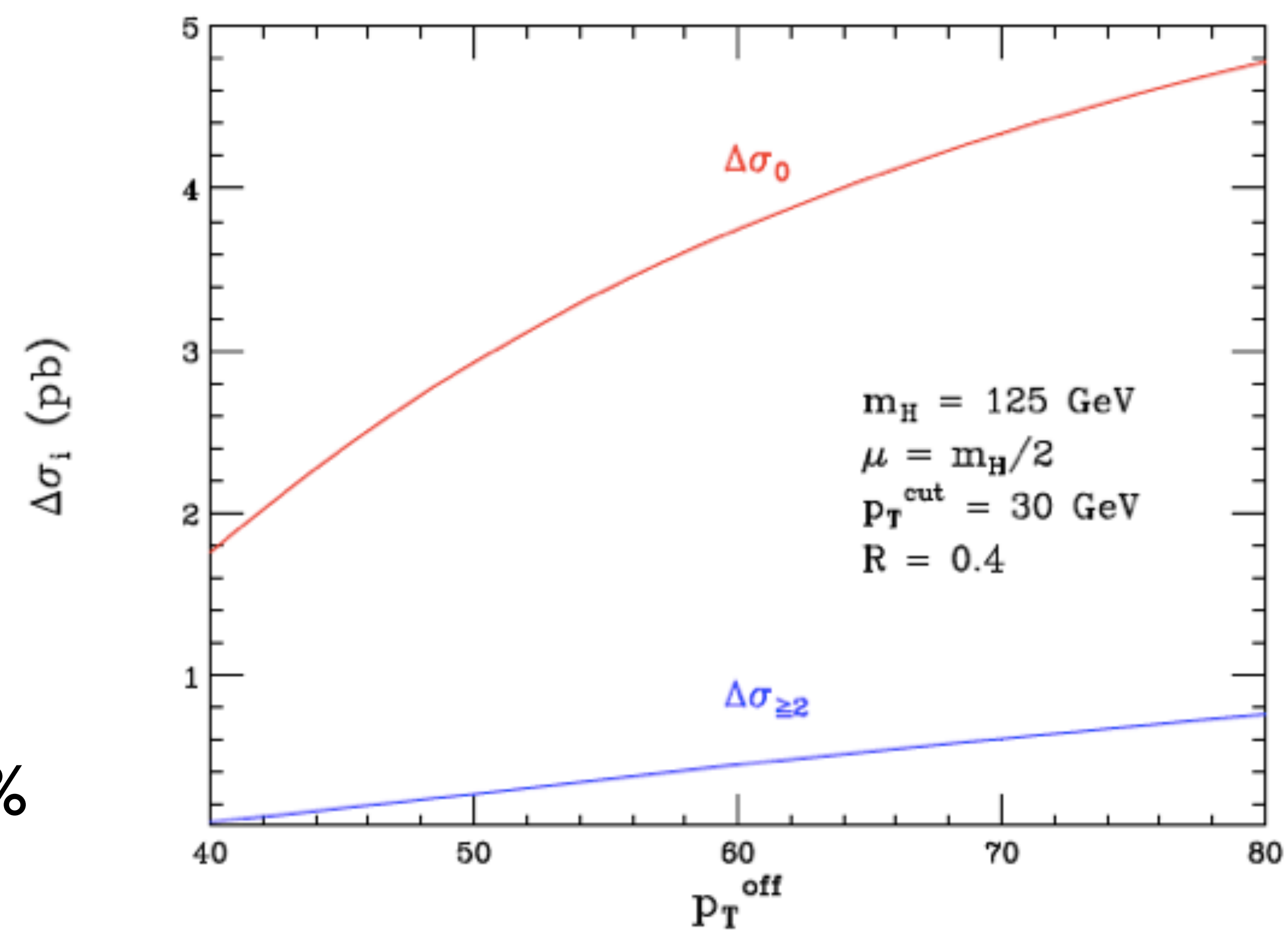

Checks of low-p_T indirect resummation

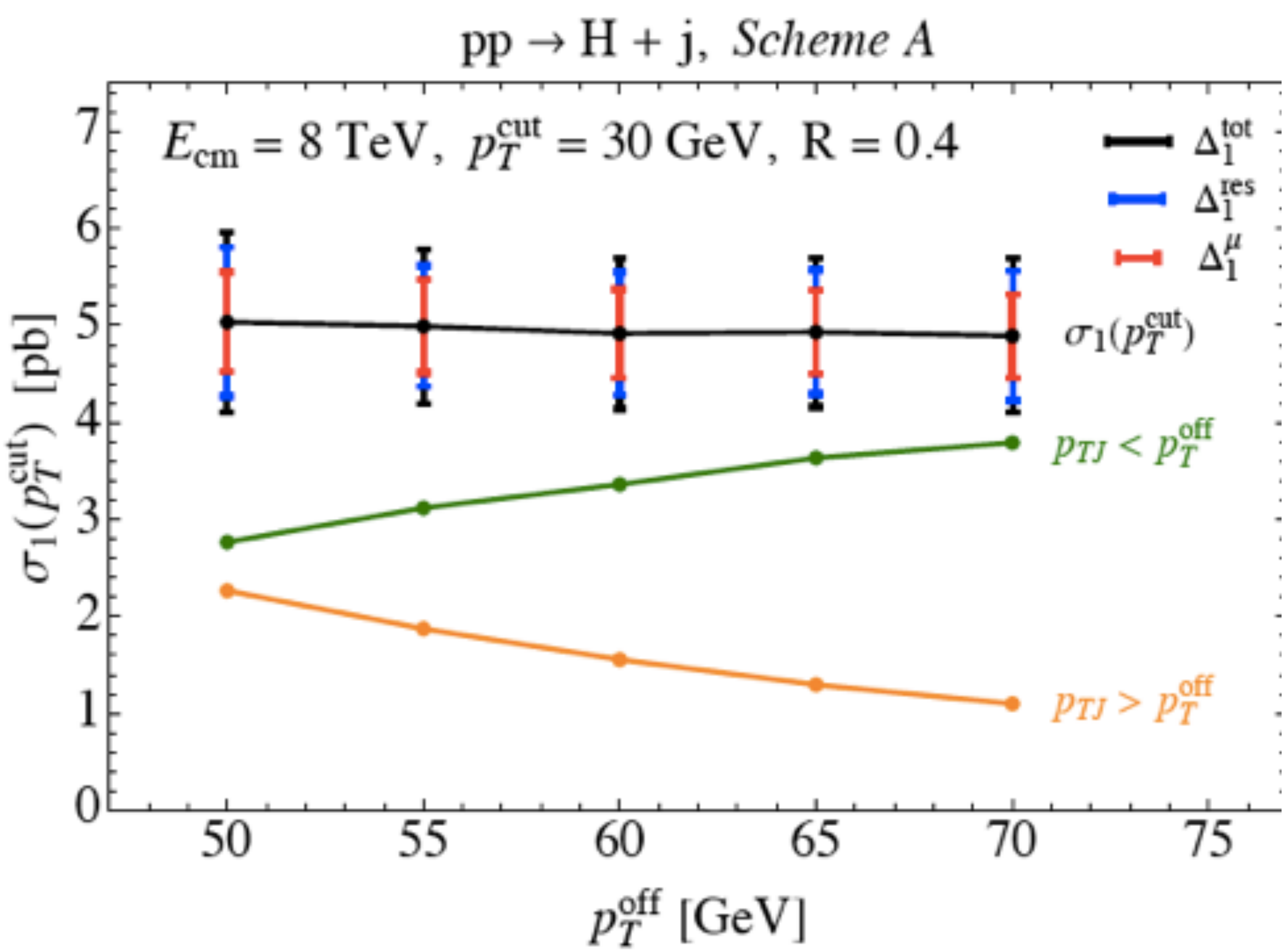

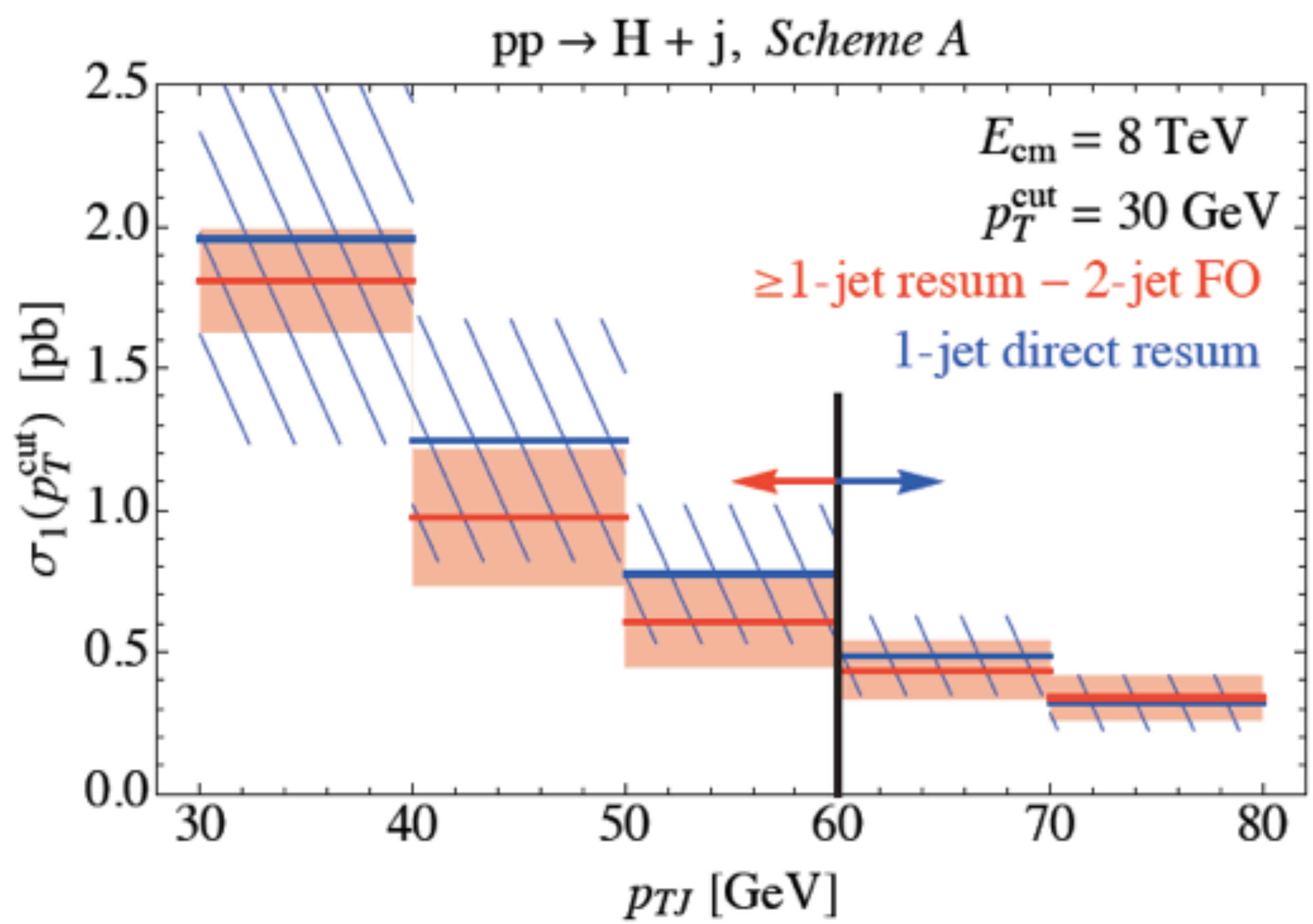

- Can check that the total 1-jet rate is insensitive to the choice of p_{off}

- Can check that the jet p_T spectrum is smooth across p_{off}, well within estimated errors

Checks of low-p_T indirect resummation

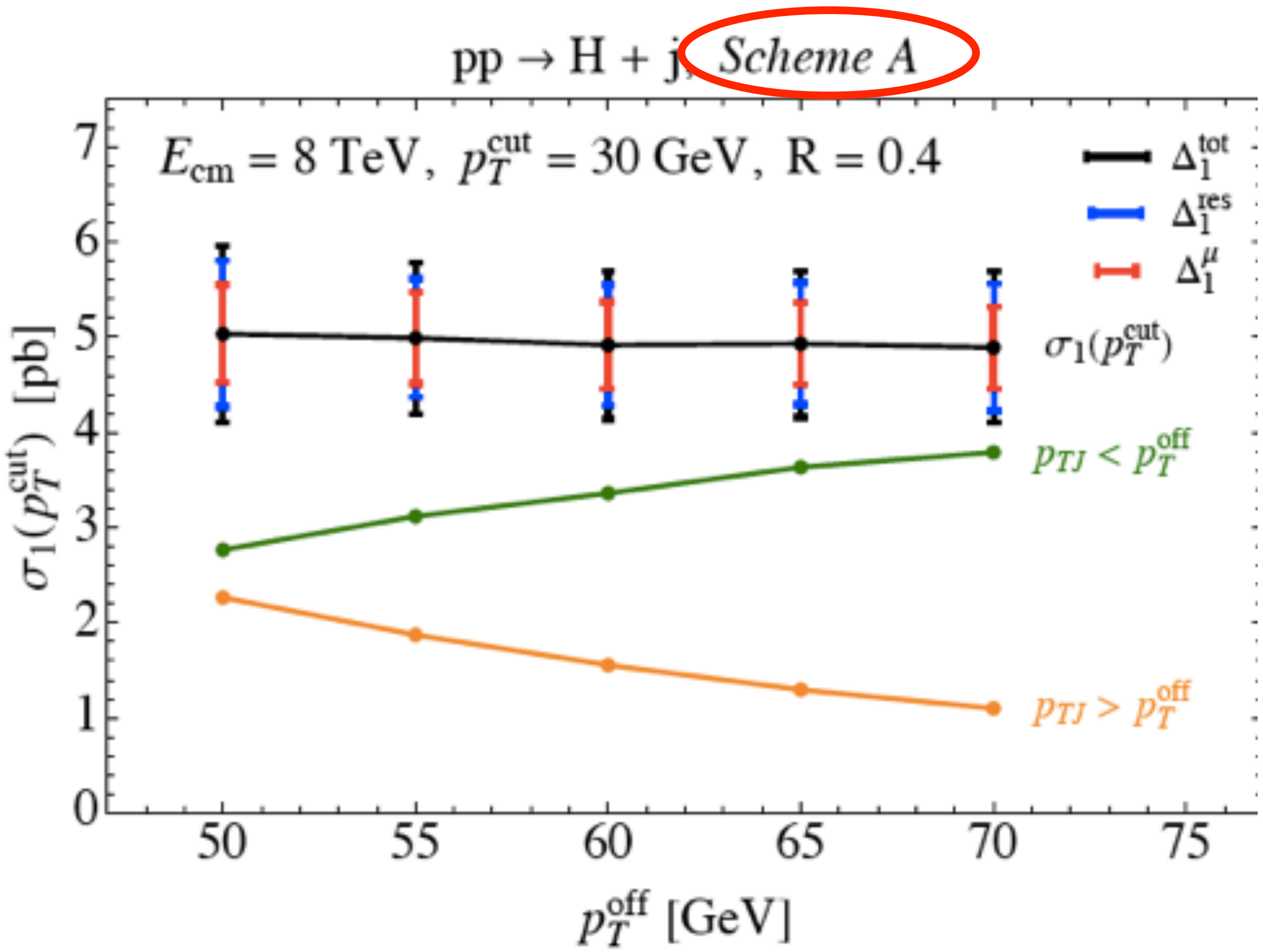

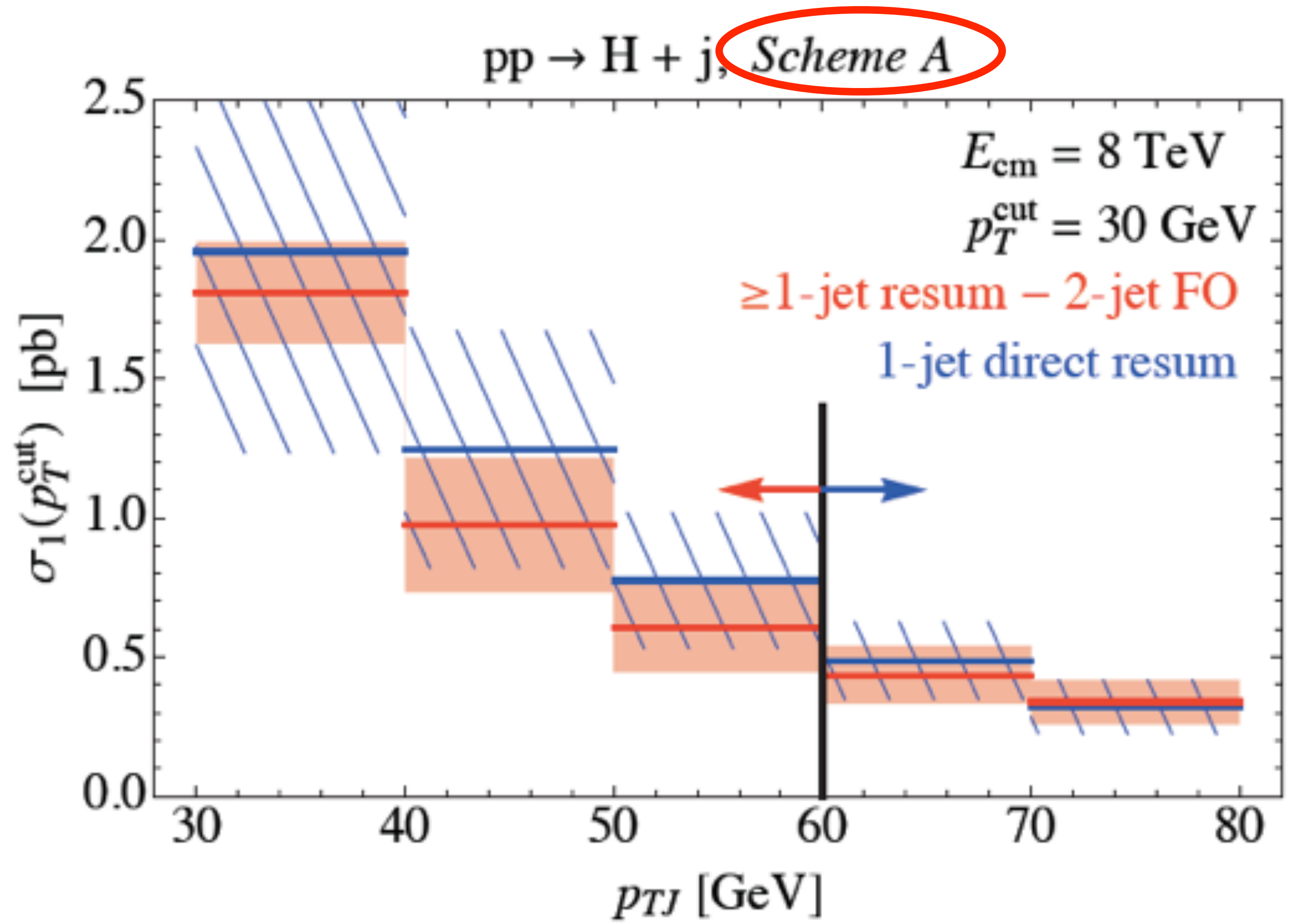

- *Scheme A*: use of an imaginary matching scale for the 0-jet cross section ("π^2 resummation), and the NNLO hard function for H+jet. Leads to a marked improvement in the matching shown above

Numerical predictions for LHC

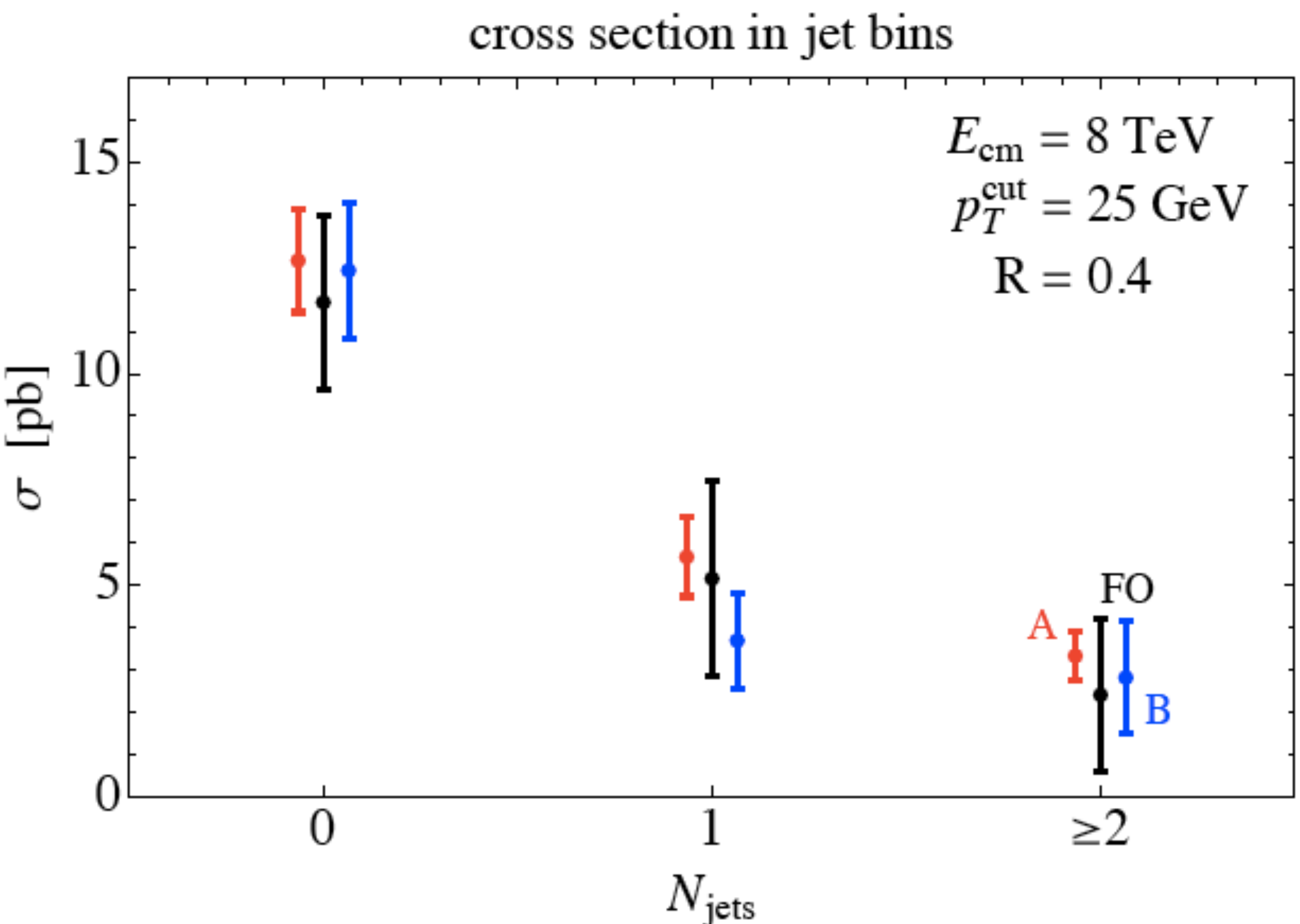

- Significant improvements in all three jet bins used in the experimental analyses (also true in *Scheme B* without imaginary matching scale)

fixed-order RG-improved

Change in the covariance matrix C(σ_0,σ_1,$\sigma_{\geq 2}$):

$$\begin{pmatrix} 4.24 & -1.99 & 0 \\ -1.99 & 5.23 & -3.24 \\ 0 & -3.24 & 3.24 \end{pmatrix} \mathrm{pb}^2 \Rightarrow \begin{pmatrix} 1.49 & -0.39 & 0.20 \\ -0.39 & 0.88 & -0.04 \\ 0.20 & -0.04 & 0.32 \end{pmatrix} \mathrm{pb}^2$$

Boughezal et al., 1312.4535

Numerical predictions for LHC

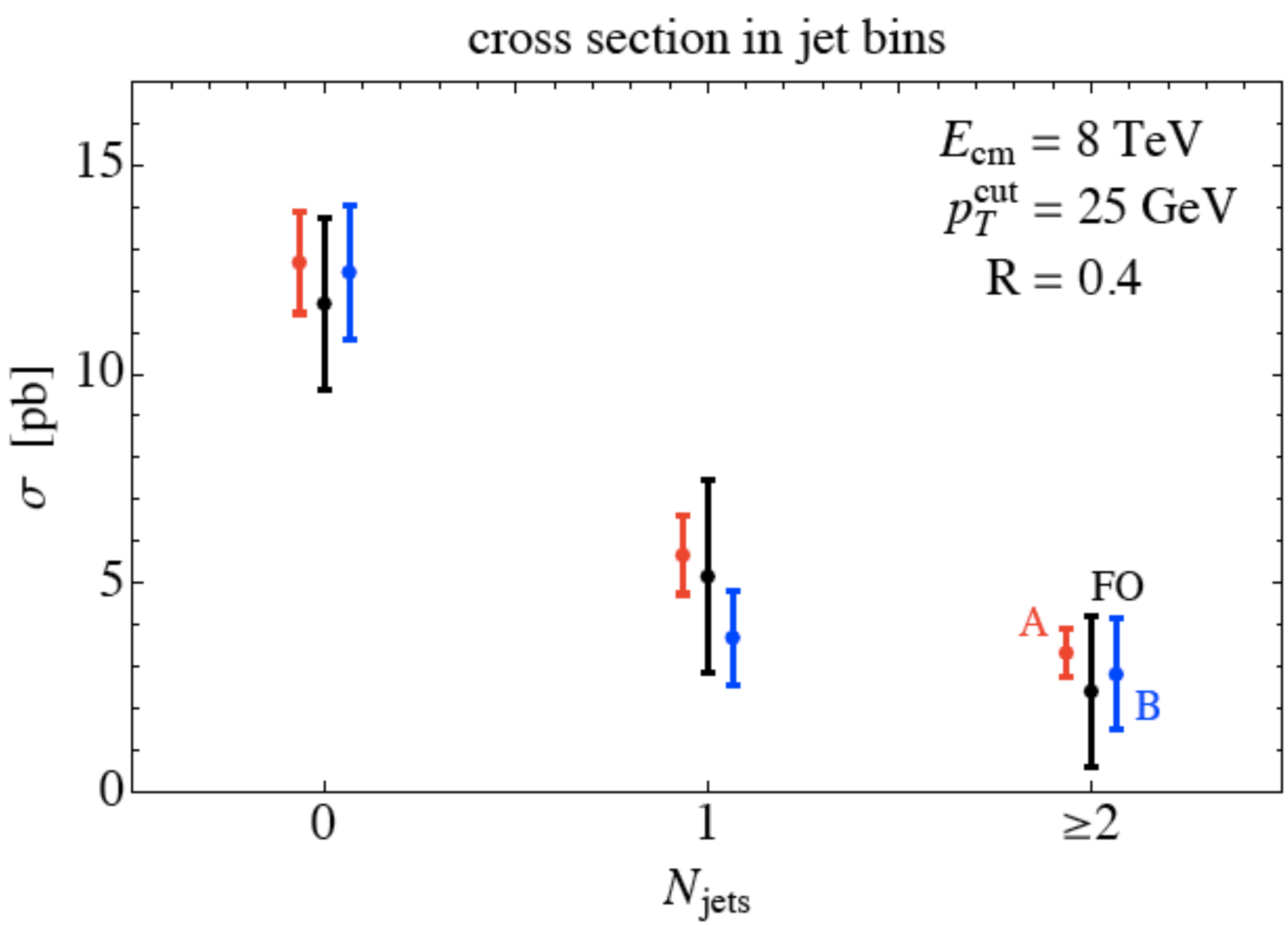

- ATLAS gives all information necessary to translate the improved covariance matrix into an improved signal-strength measurement

$(\Delta\mu/\mu)_{FO}$ = 13.3%

$(\Delta\mu/\mu)_{RG}$ = 6.9%

- Fixed-order result consistent with ATLAS finding
- Nearly a factor of 2 reduction in theory uncertainty in the WW channel!

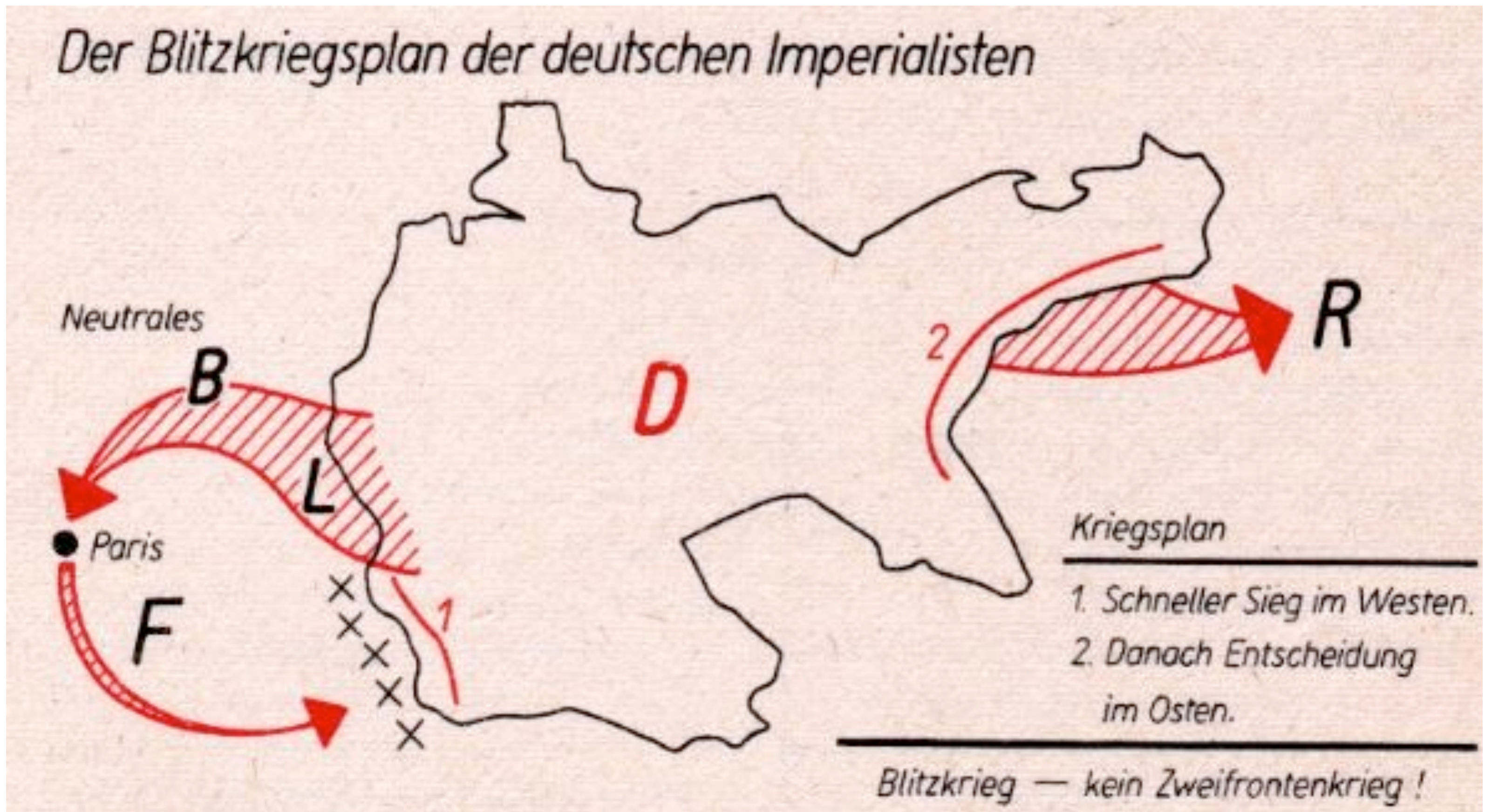

Higgs plus jet at NNLO

Need for H+j @ NNLO

- Although resummation can help tame these large logs, need further fixed-order progress... relevant kinematics is in the transition region between resummation and fixed order

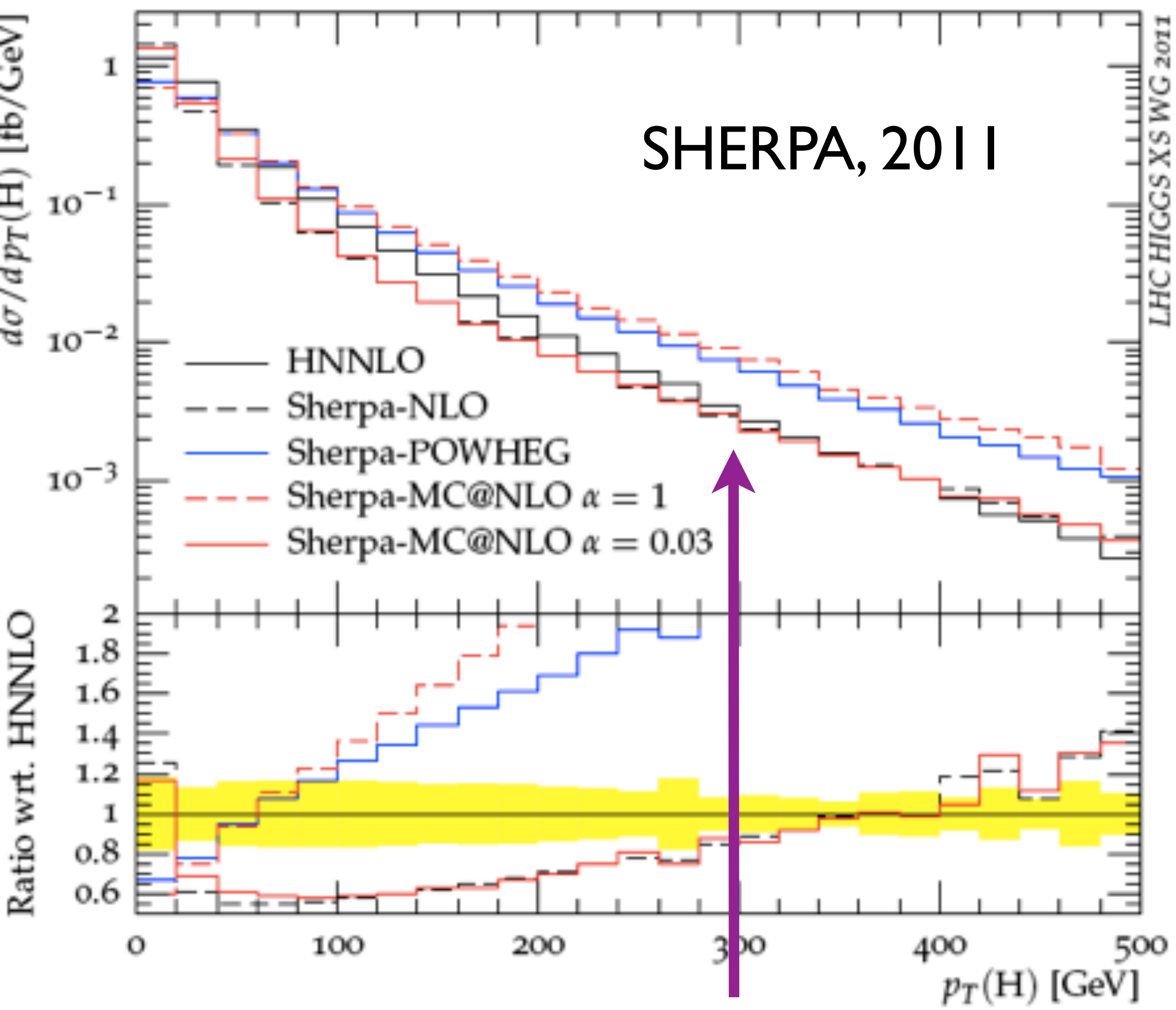

Large differences in NLO+PS p_T spectra need NNLO to resolve

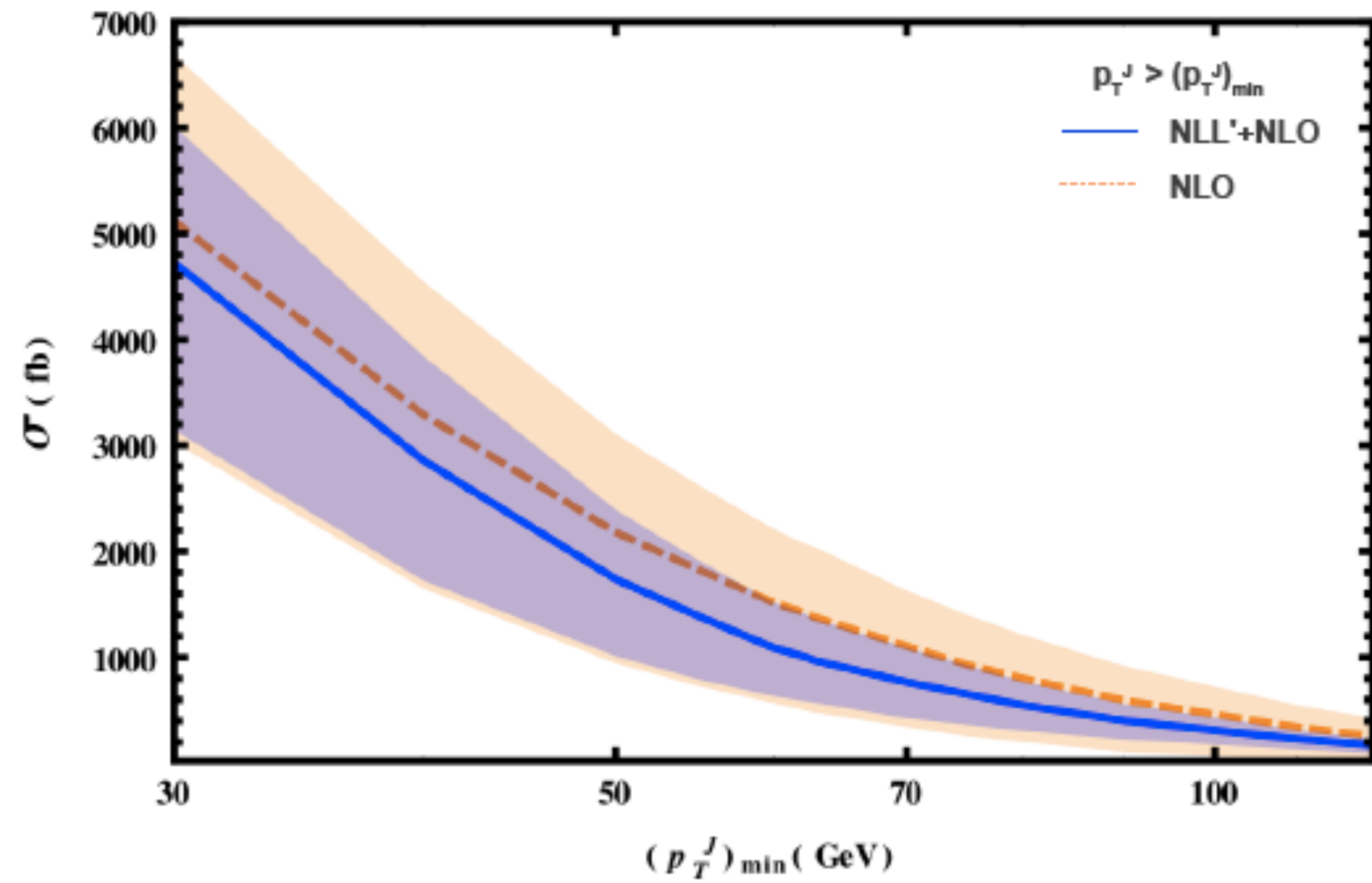

Need NNLO H+jet to extend the accuracy of the resummation just discussed

Structure of NNLO cross section

- Need the following ingredients for a NNLO cross section

2-loop matrix elements, m partons

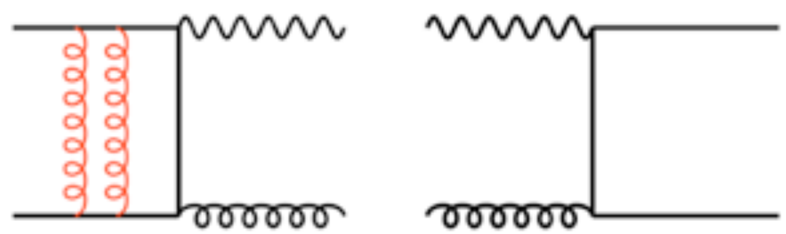

- Explicit IR poles from loop integrals

1-loop matrix elements, m+1 partons

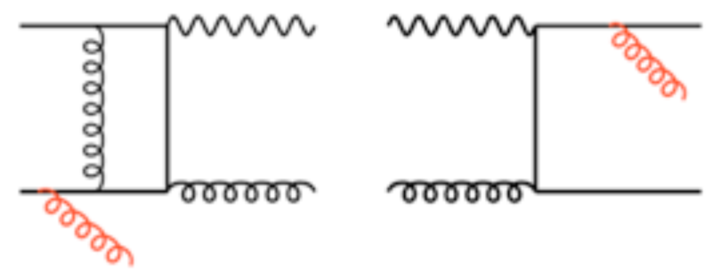

- Explicit IR poles from loops
- Implicit IR poles from single unresolved radiation

Tree level matrix elements, m+2 partons

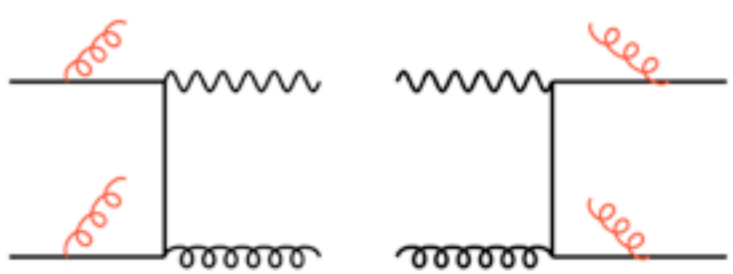

Implicit IR poles from double unresolved radiation

- IR singularities cancel in the sum of real and virtual corrections and mass factorization counterterms but only after phase space integration for real radiations
- Need a procedure to extract poles before phase-space integration to allow for differential observables

How to calculate at NLO

- Well-honed techniques for calculating and combining real+virtual at NLO
- Virtual corrections with Feynman diagrams or new unitarity techniques (
- To deal with IR singularities of real emission, have dipole subtraction, FKS subtraction

$$d\sigma_{NLO} = \int_{d\Phi_{m+1}} \left(d\sigma^R_{NLO} - d\sigma^S_{NLO}\right) + \left[\int_{d\Phi_{m+1}} d\sigma^S_{NLO} + \int_{d\Phi_m} d\sigma^V_{NLO}\right]$$

Approximates real-emission matrix elements in all singular limits so this difference is numerically integrable

Simple enough to integrate analytically so that 1/ε poles can be cancelled against virtual corrections

Subtraction at NNLO

- The generic form of an NNLO subtraction scheme is the following:

$$
\begin{aligned}
d\sigma_{NNLO} = & \int_{d\Phi_{m+2}} \left(d\sigma^{R}_{NNLO} - d\sigma^{S}_{NNLO} \right) \\
& + \int_{d\Phi_{m+1}} \left(d\sigma^{V,1}_{NNLO} - d\sigma^{VS,1}_{NNLO} \right) \\
& + \int_{d\Phi_{m+2}} d\sigma^{S}_{NNLO} + \int_{d\Phi_{m+1}} d\sigma^{VS,1}_{NNLO} \\
& + \int_{d\Phi_{m}} d\sigma^{V,2}_{NNLO} ,
\end{aligned}
$$

- Maximally singular configurations at NNLO can have two collinear, two soft singularities
- Subtraction terms must account for all of the many possible singular configurations: triple-collinear ($p_1||p_2||p_3$), double-collinear ($p_1||p_2,p_3||p_4$), double-soft, single-soft, soft +collinear, etc.

- The factorization of the matrix elements in all singular configurations is known in the literature

The triple-collinear example

- To illustrate the problems that occur when trying to use these formulae, consider the triple-gluon collinear limit. The factorization of the matrix element squared in this limit is the following.

$$|\mathcal{M}(\ldots,p_1,p_1,p_3)|^2 \approx \frac{4g_s^4}{s_{123}^2}\mathcal{M}^\mu(\ldots,p_1+p_2+p_3)\mathcal{M}^{\nu *}(\ldots,p_1+p_2+p_3)\,P^{\mu\nu}_{g_1g_2g_3}$$

$z_i = E_i/(\sum E_j)$

$$\begin{aligned}
\hat{P}^{\mu\nu}_{g_1g_2g_3} &= C_A^2 \left\{ \frac{(1-\epsilon)}{4s_{12}^2}\left[-g^{\mu\nu}t_{12,3}^2 + 16 s_{123}\frac{z_1^2 z_2^2}{z_3(1-z_3)}\left(\frac{\widetilde{k}_2}{z_2}-\frac{\widetilde{k}_1}{z_1}\right)^\mu \left(\frac{\widetilde{k}_2}{z_2}-\frac{\widetilde{k}_1}{z_1}\right)^\nu \right]\right. \\
&- \frac{3}{4}(1-\epsilon)g^{\mu\nu} + \frac{s_{123}}{s_{12}}g^{\mu\nu}\frac{1}{z_3}\left[\frac{2(1-z_3)+4z_3^2}{1-z_3} - \frac{1-2z_3(1-z_3)}{z_1(1-z_1)}\right] \\
&+ \frac{s_{123}(1-\epsilon)}{s_{12}s_{13}}\left[2z_1\left(\widetilde{k}_2^\mu\widetilde{k}_2^\nu\frac{1-2z_3}{z_3(1-z_3)} + \widetilde{k}_3^\mu\widetilde{k}_3^\nu\frac{1-2z_2}{z_2(1-z_2)}\right)\right. \\
&+ \frac{s_{123}}{2(1-\epsilon)}g^{\mu\nu}\left(\frac{4z_2z_3+2z_1(1-z_1)-1}{(1-z_2)(1-z_3)} - \frac{1-2z_1(1-z_1)}{z_2z_3}\right) \\
&+ \left.\left.\left(\widetilde{k}_2^\mu\widetilde{k}_3^\nu + \widetilde{k}_3^\mu\widetilde{k}_2^\nu\right)\left(\frac{2z_2(1-z_2)}{z_3(1-z_3)} - 3\right)\right]\right\} + (5 \text{ permutations}) \;.
\end{aligned}$$

Catani, Grazzini 1999

Entangled singularities

- To illustrate the problems that occur when trying to use these formulae, consider the triple-gluon collinear limit. The factorization of the matrix element squared in this limit is the following.

$$|\mathcal{M}(\ldots,p_1,p_1,p_3)|^2 \approx \frac{4g_s^4}{s_{123}^2}\mathcal{M}^{\mu}(\ldots,p_1+p_2+p_3)\mathcal{M}^{\nu *}(\ldots,p_1+p_2+p_3)\,P^{\mu\nu}_{g_1 g_2 g_3}$$

- When one introduces an explicit parameterization:

$s_{123} \sim E_1E_2(1-c_{12})+E_1E_3(1-c_{13})+E_2E_3(1-c_{23})$

- What goes to zero quicker? E_1,E_2,E_3,$(1-c_{12})$,$(1-c_{13})$, or $(1-c_{23})$?
- Need to order the limits, since singularities must be extracted from integrals of the schematic form:

$$\int_0^1 dx dy \frac{x^{\epsilon}y^{\epsilon}}{(x+y)^2}F_J(x,y)$$

- Need a systematic technique for ordering limits, too many of such issues appear

Sector decomposition

- Can define a systematic procedure to order limits

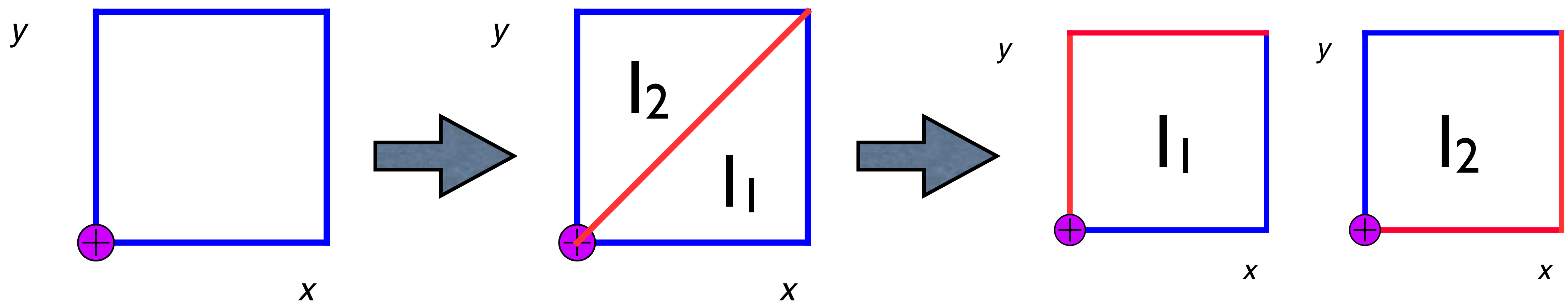

$$I = \int_0^1 \mathrm{d}x\mathrm{d}y \frac{x^\epsilon y^\epsilon}{(x+y)^2}$$

$$I_1 = \int_0^1 \mathrm{d}x \int_0^x \mathrm{d}y \frac{x^\epsilon y^\epsilon}{(x+y)^2} \qquad I_1 = \int_0^1 \mathrm{d}x\mathrm{d}y \frac{x^{-1+2\epsilon} y^\epsilon}{(1+y)^2}$$

$$I_2 = \int_0^1 \mathrm{d}y \int_0^y \mathrm{d}x \frac{x^\epsilon y^\epsilon}{(x+y)^2} \qquad I_2 = \int_0^1 \mathrm{d}x\mathrm{d}y \frac{y^{-1+2\epsilon} x^\epsilon}{(1+x)^2}$$

$$y^{-1-\epsilon} = -\frac{\delta(y)}{\epsilon} + \left[\frac{1}{y}\right]_+ - \epsilon \left[\frac{\ln y}{y}\right]_+ + \mathcal{O}(\epsilon^2)$$

Binoth, Heinrich; Anastasiou, Melnikov, FP 2003-2005

Sector decomposition

- Give up on the idea of analytic cancellation of poles; calculate the coefficients of $1/\varepsilon^n$ Laurent expansion numerically
- In its original incarnation, was applied directly to each interference of diagrams which appears.
- Used for the first differential NNLO calculations at hadron colliders: Higgs, W/Z
- The (major) drawback: originally used a *global* phase-space parameterization for a given interference

Higgs production

- To illustrate the drawbacks, use Higgs production as an example. Consider one of the diagrammatic contributions to the double-real radiation correction.

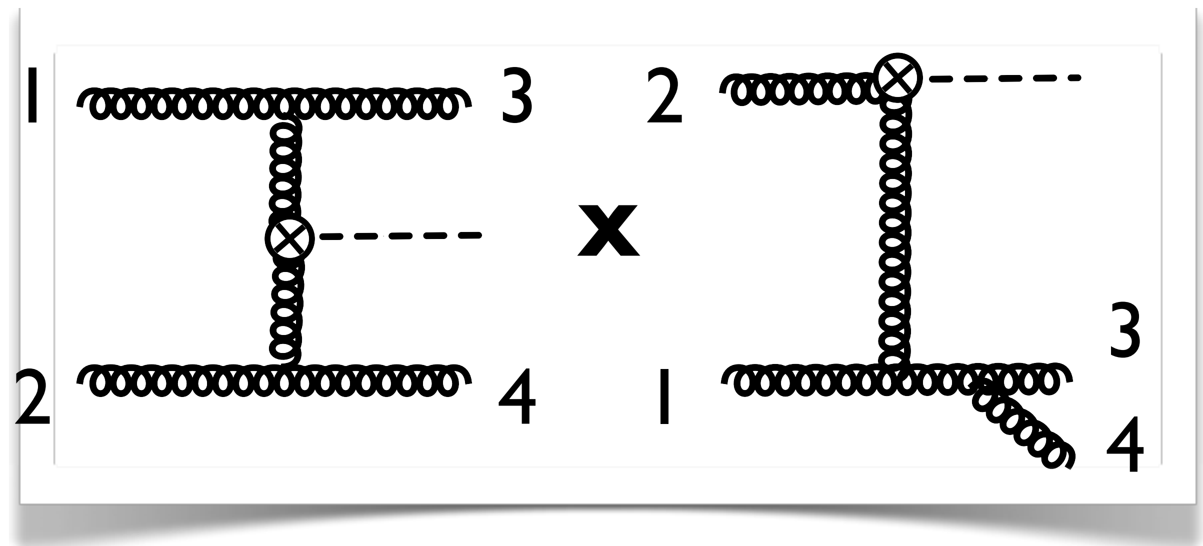

- Invariants that occur in this topology : s_{13}, s_{24}, s_{134}, s_{34}. These contain collinear singularities $p_1||p_3$, $p_2||p_4$, $p_3||p_4$, $p_1||p_3||p_4$
- The structure of these singularities makes it difficult to find a suitable global parameterization amenable to sector decomposition.
- Would need to start over with entirely new parameterization for Higgs+jet
- However, can only have $p_1||p_3$ & $p_2||p_4$ or $p_1||p_3||p_4$ in a given phase space region. Not all invariants above can have collinear singularities simultaneously.

FKS@NNLO

- Key idea: pre-partitioning of the phase space leads to a phase-space parameterization applicable to NNLO real-radiation corrections for any process, regardless of multiplicity (Czakon, 2010).
- Partition the phase space such that in each partition only a subset of particles leads to singularities, and only one triple collinear or one double collinear singularity can occur. This is effectively an extension of the FKS subtraction technique to NNLO.
- Allows use of known soft/collinear limits, and is extendable to higher multiplicity. Let's see these points explicitly in a simple test case.

Z decay at NNLO in QED

- We will illustrate the details with $Z\rightarrow e^+e^-$ to NNLO in QED (Boughezal, Melnikov, FP 2011). Retains the features of the QCD computation, but makes the formulae a bit simpler to show.
- Study the double-real radiation correction: $Z\rightarrow e^+(p_+)e(p_-)\gamma(p_1)\gamma(p_2)$
- The starting point is the partitioning of phase space:

$$1 = \delta_{12}^{--} + \delta_{12}^{++} + \delta_{12}^{-+} + \delta_{12}^{+-}$$

$$\delta_{12}^{--} = \frac{1-\hat{n}_1\cdot\hat{n}_+}{2-\hat{n}_1\cdot\hat{n}_+-\hat{n}_1\cdot\hat{n}_-}\,\frac{1-\hat{n}_2\cdot\hat{n}_+}{2-\hat{n}_2\cdot\hat{n}_+-\hat{n}_2\cdot\hat{n}_-}$$

- Focus on this triple-collinear partition as an example. Has only p_1,p_2 soft and $p_1||p_2||p_-$. We don't care how ugly the invariants s_{1+},s_{2+} are. They contain no collinear singularities, only (simple) energy singularities.

The triple-collinear decomposition

- The most complicated invariant appearing in this partition is s_{-12}

$$s_{-12} \sim A\xi_1\eta_1 + B\xi_2\eta_2 + C\xi_1\xi_2(\eta_1-\eta_2)^2$$

$$\cos\theta_i = 1-2\eta_i$$
$$E_i = \xi_i M_Z/2$$

- Perform the following sector decompositions to disentangle singularities

  - Order energies, focus on $\xi_1 > \xi_2$, $\xi_2 \rightarrow \xi_1\xi_2$

    $$s_{-12} \sim \xi_1(A\eta_1 + B\xi_2\eta_2 + C\xi_1\xi_2(\eta_1-\eta_2)^2)$$

  - Order angles, focus on $\eta_2 > \eta_1$, $\eta_1 \rightarrow \eta_1\eta_2$

    $$s_{-12} \sim \xi_1\eta_2(A\eta_1 + B\xi_2 + C\xi_1\xi_2\eta_2(1-\eta_1)^2)$$

  - Order η_1,ξ_2, focus on $\eta_1 > \xi_2$, $\xi_2 \rightarrow \xi_2\eta_1$

    $$s_{-12} \sim \xi_1\eta_2\eta_1(A + B\xi_2 + C\xi_1\xi_2\eta_2(1-\eta_1)^2)$$

All singularities extracted as overall multiplicative factors

Bracket is finite in all limits

The triple-collinear decomposition

- We're left with the following variable changes to factorize singularities

1. S_1^{--}, where $\xi_1 = x_1$, $\xi_2 = x_{\max} x_2 x_1$, $\eta_1 = x_3$, $\eta_2 = x_4 x_3$, $\kappa = x_5$;
2. S_2^{--}, where $\xi_1 = x_1$, $\xi_2 = x_{\max} x_2 x_4 x_1$, $\eta_1 = x_3 x_4$, $\eta_2 = x_3$, $\kappa = x_5$;
3. S_3^{--}, where $\xi_1 = x_1$, $\xi_2 = x_{\max} x_2 x_1$, $\eta_1 = x_2 x_3 x_4$, $\eta_2 = x_3$, $\kappa = x_5$.

Crucial point: sectors are identical for *any* NNLO QED correction. Just as we didn't care about the form of s_{1+}, s_{2+}, we don't care about s_{1j}, s_{2j} in this partition, where j indicates any other particle we add to the process. We are working with a *local* parameterization suitable for any triple-collinear partition.

For sector S_1^{--}:

$$\boxed{E_1 = \frac{m_Z}{2} x_1, \quad E_2 = \frac{m_Z}{2} x_1 x_2 x_{\max},}$$

$$\boxed{\cos\theta_1 = 1 - 2x_3, \quad \cos\theta_2 = 1 - 2x_3 x_4.}$$

The triple-collinear decomposition

- We have reduced our calculation to the following objects:

$$\int \mathrm{d}\underline{\mathrm{Lips}}^{--}_{S_1} F_1(x_1, x_2, x_3, x_4, x_5)$$

with

regular functions of x_i

$$\mathrm{d}\underline{\mathrm{Lips}}^{--}_{S_1} = \mathrm{dNorm}\ \mathrm{PS}_w\ \ (\mathrm{PS})^{-\epsilon} \times \frac{\mathrm{d}x_1}{x_1^{1+4\epsilon}} \frac{\mathrm{d}x_2}{x_2^{1+2\epsilon}} \frac{\mathrm{d}x_3}{x_3^{1+2\epsilon}} \frac{\mathrm{d}x_4}{x_4^{1+\epsilon}} \frac{\mathrm{d}\kappa}{\pi(\kappa(1-\kappa))^{1/2}}$$

expandable in plus distributions

and

$$F_1(\{x_{i=1..5}\}) = \left[x_1^4 x_2^2 x_3^2 x_4 m_Z^2 \delta_{12}^{--}\right] |\mathcal{M}_{Z\to e^+e^-\gamma\gamma}|^2$$

Let's look at some of the singularities that can occur

The double-soft limit

$$E_1 = \frac{m_Z}{2} x_1, \quad E_2 = \frac{m_Z}{2} x_1 x_2 x_{\max},$$

$$\cos\theta_1 = 1 - 2x_3, \quad \cos\theta_2 = 1 - 2x_3 x_4.$$

- What happens if $x_1 = 0$? ⟹ $E_1 = E_2 = 0$ ⟹ double soft limit

the QED matrix element factorizes completely, use known singular limits

$$|\mathcal{M}_{Z\to e^+e^-\gamma\gamma}|^2 \to e^4 J_1 J_2 |\mathcal{M}_{Z\to e^-e^+}|^2$$

with

$$J_i = \frac{2p_- \cdot p_+}{(p_- \cdot p_i)(p_+ \cdot p_i)}$$

derive the following formula

$$F_1|_{x_1=0} = \frac{16e^4}{m_Z^2} |\mathcal{M}_{Z\to e^-e^+}|^2$$

easy to calculate numerically

The soft+collinear limit

$$E_1 = \frac{m_Z}{2} x_1, \quad E_2 = \frac{m_Z}{2} x_1 x_2 x_{\max},$$

$$\cos\theta_1 = 1 - 2x_3, \quad \cos\theta_2 = 1 - 2x_3 x_4.$$

- What happens if $x_2 = 0$ & $x_3 = 0$? → $E_2 = 0$ & $p_1 \parallel p_-$ → soft-collinear limit

The matrix element factorizes in two steps:

soft factorization of γ_2 $\quad |\mathcal{M}_{Z\to e^+e^-\gamma_1\gamma_2}|^2 \to e^2 J_2 |\mathcal{M}_{Z\to e^+e^-\gamma_1}|^2$

collinear factorization of γ_1 $\quad |\mathcal{M}_{Z\to e^+e^-\gamma_1}|^2 \approx \frac{2e^2}{s_{1e}} P_{e\gamma}(\epsilon, z) |\mathcal{M}_{Z\to e^+\tilde{e}^-}|^2$

derive the following formula

$$F_1|_{x_2=0,x_3=0} = \frac{16e^4 x_1}{m_Z E_- x_{\max}^2 \Delta_{12}} P_{e\gamma}(\epsilon, z) \times |\mathcal{M}_{Z\to e^+\tilde{e}^-}|^2.$$

easy to calculate numerically

Moving onto Higgs+jet

- What differences occur when considering a more complex process such as Higgs+jet? Let's look at the double-real radiation.
- First introduce a transverse-momentum partitioning to ensure that at least one hard parton is in the final state:

$$\Delta = \frac{p_{T3}}{p_{T3} + p_{T4} + p_{T5}}$$

- Perform an angular partitioning similar to that for $Z \to e^+e^-$
- Left with the following partitions: $p_5||p_4||p_1$, $p_5||p_4||p_2$, $p_5||p_4||p_3$, $p_5||p_1\&p_4||p_2$, $p_5||p_2\&p_4||p_1$, $p_5||p_1\&p_4||p_3$, $p_5||p_3\&p_4||p_1$, $p_5||p_2\&p_4||p_3$, $p_5||p_3\&p_4||p_2$

Sector structure

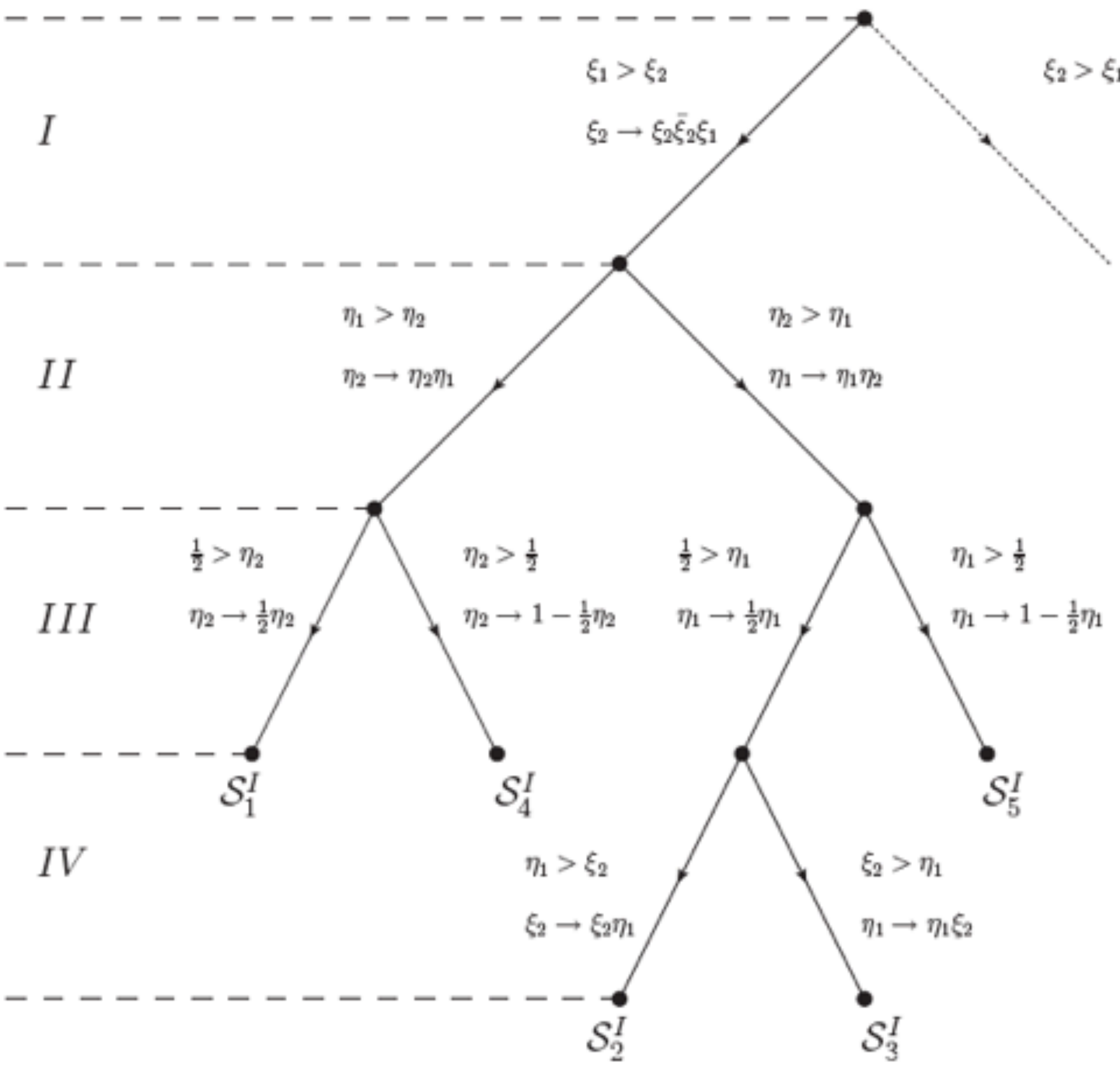

- Follow same procedure as for the QED example
- Five sectors for the triple-collinear partition, not three as in QED, from $g \to gg$ splitting
- This same sector tree applies to all three triple-collinear partitions
- Very helpful to use rotational invariance to use different reference frames in each partition. For $p_5||p_4||p_1$ set $p_1=E_1(1,0,0,1)$. For $p_5||p_4||p_3$, rotate and set $p_3=E_3(1,0,0,1)$.

Numerical setup

LO and NLO:

- gg ~ 70% full result
- qg ~ 30% full result
- qq is negligible
- pattern persists for Hjj@NLO (qq~2%) (same ingredients of Hj@NNLO)

At NNLO, we ONLY CONSIDER GG AND QG

- we must compute everything at NLO, as all channels mix under PDF renormalization

Pole cancellation at 1/ε

Numerical Cancellation between renormalization and coll. couterterms, RR, RV, VV

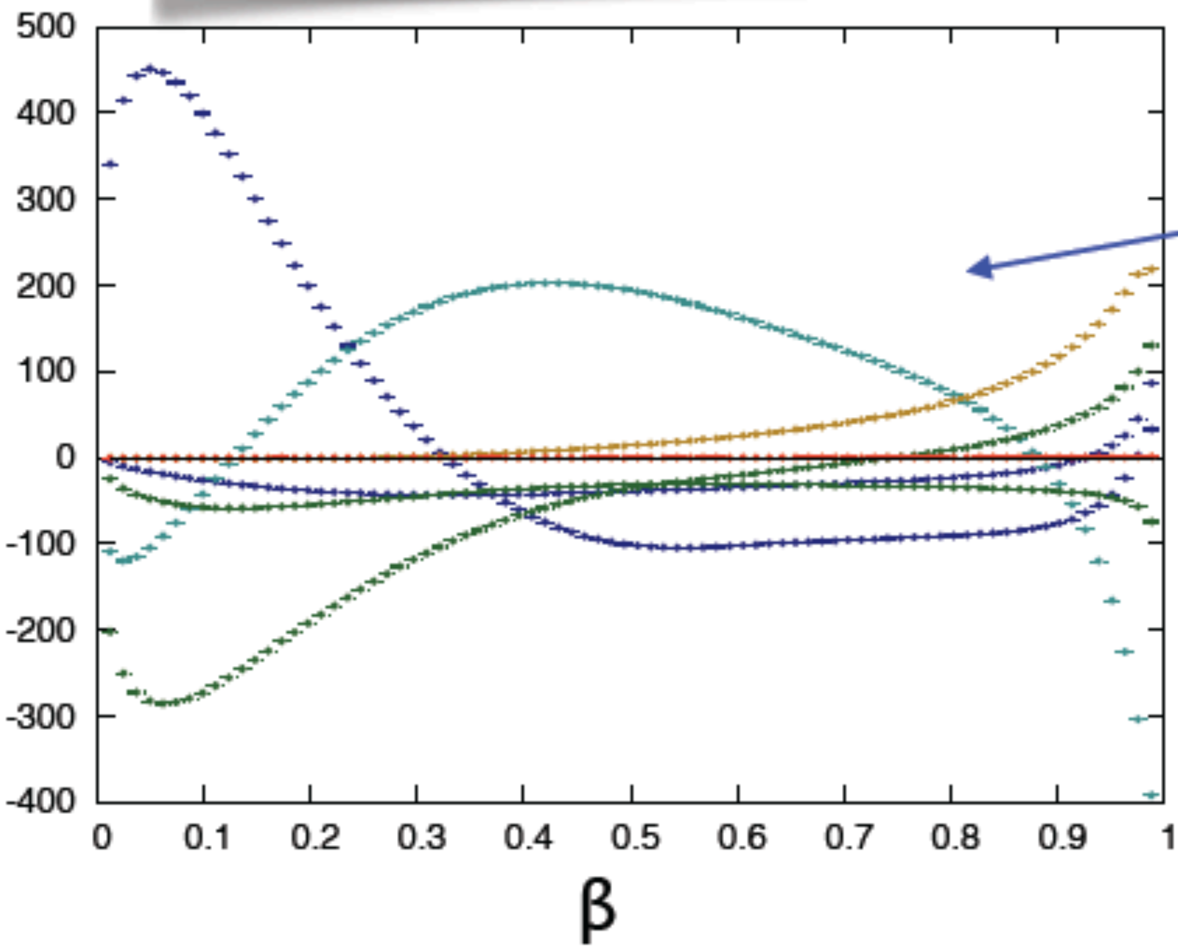

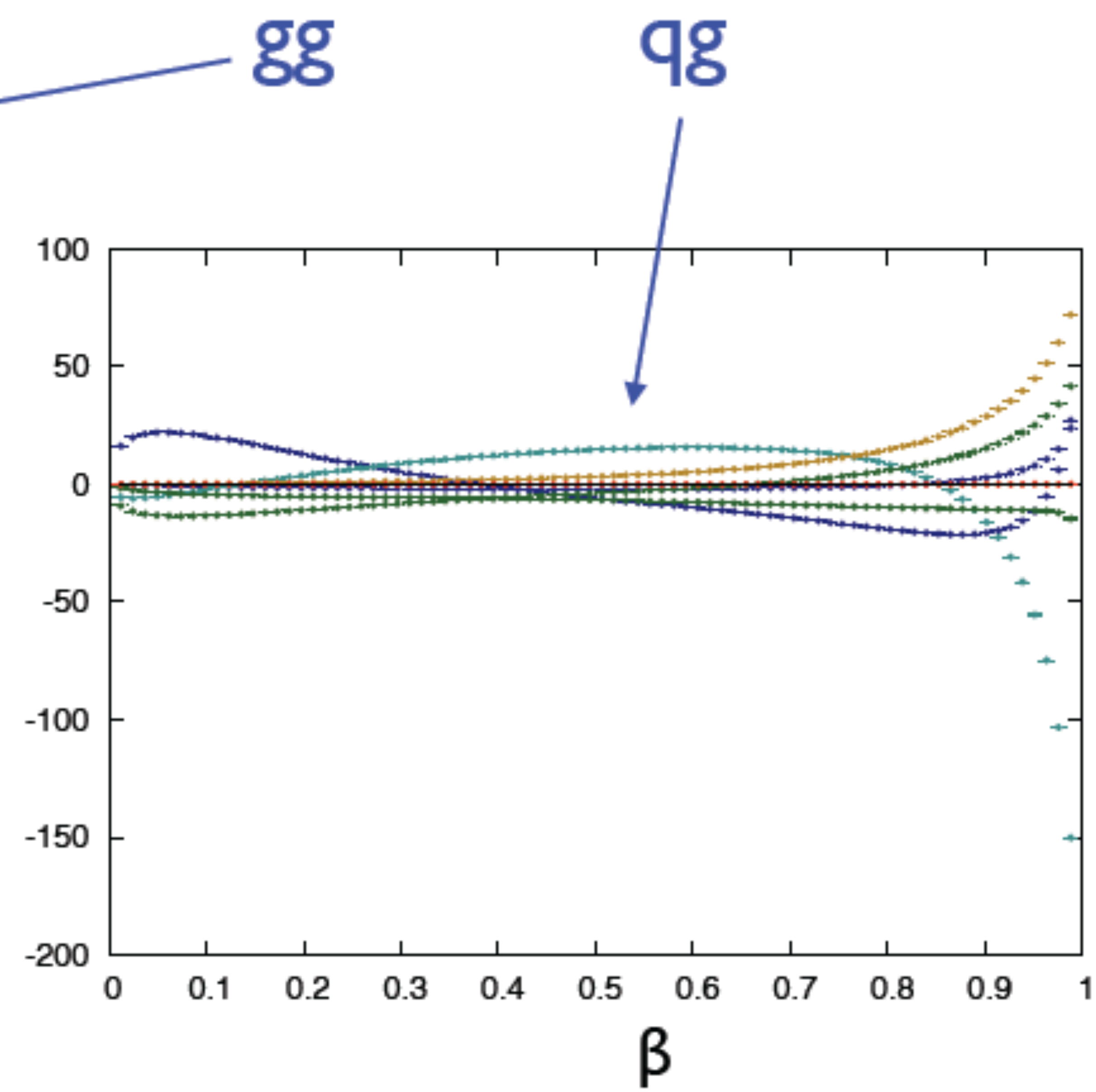

$$\beta = \sqrt{1 - \frac{s_{th}}{\hat{s}}}$$

gg numerics

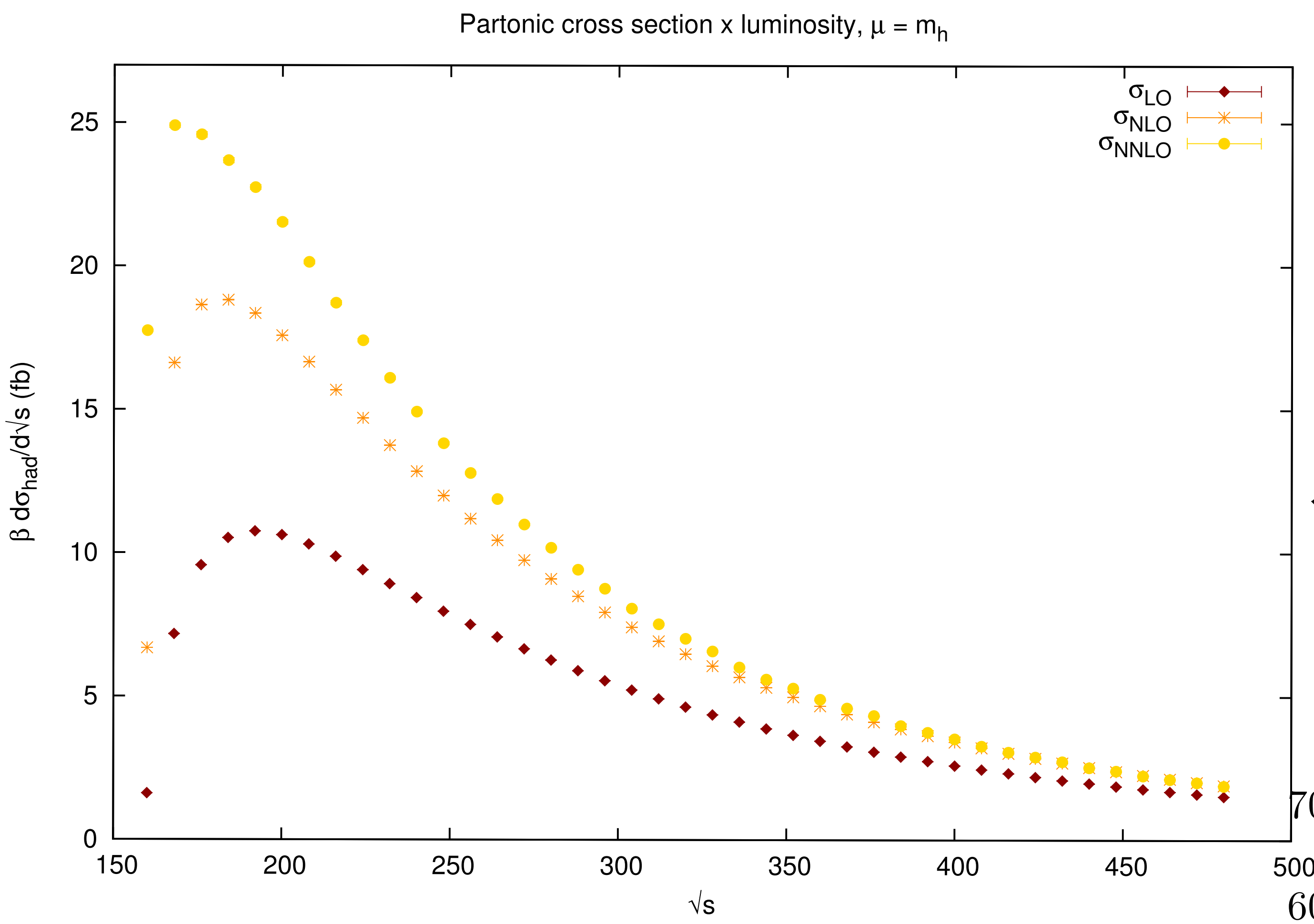

Numerics: gg channel at NNLO, $N_F=0$; k_T jets with R=0.5; NNPDF 2.3; $\mu=m_h$

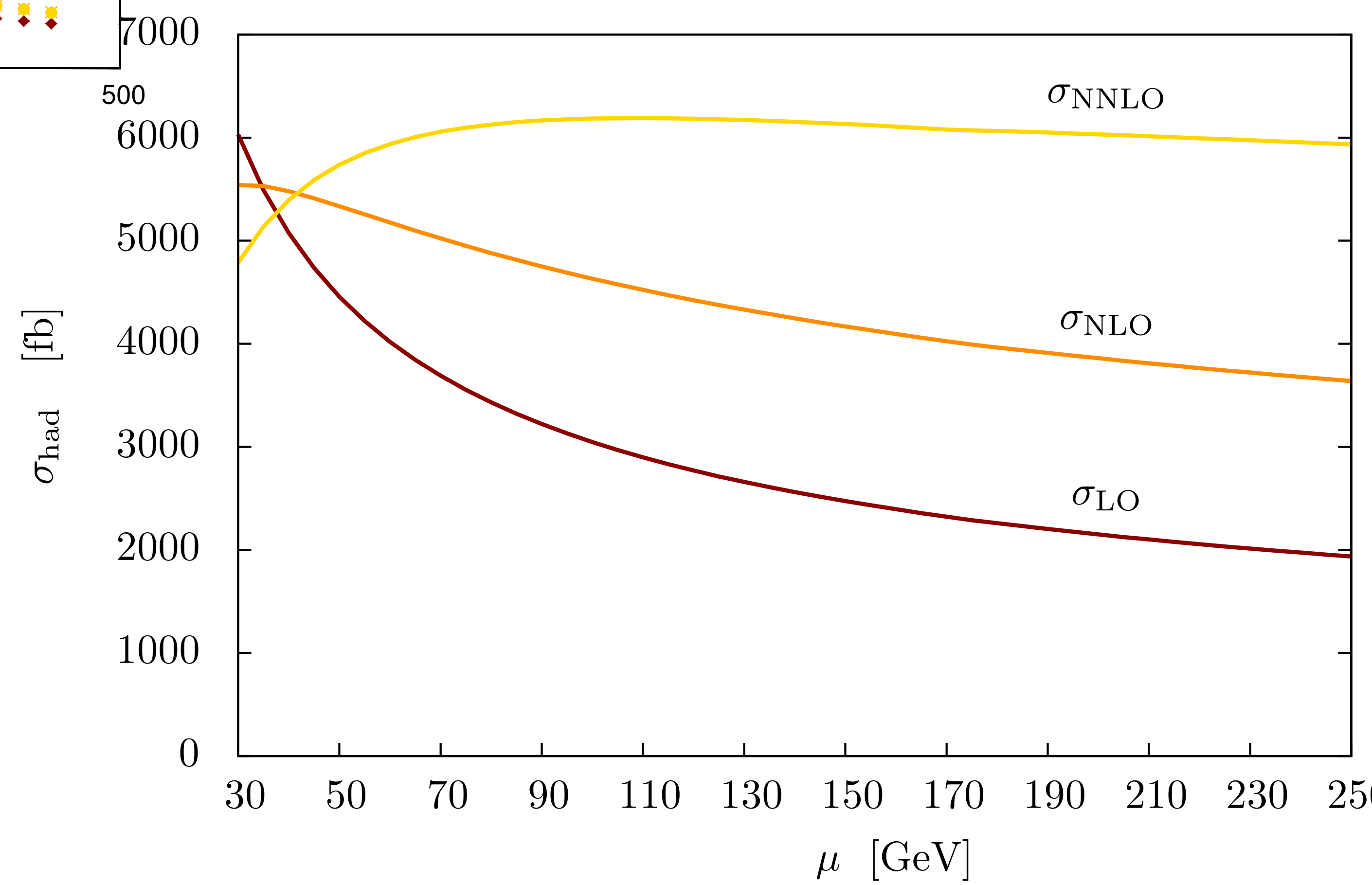

Numerical results

Numerics: gg+qg channels at NNLO, qq at NLO; anti-k_T jets with R=0.5; NNPDF 2.3; $\mu=m_h$

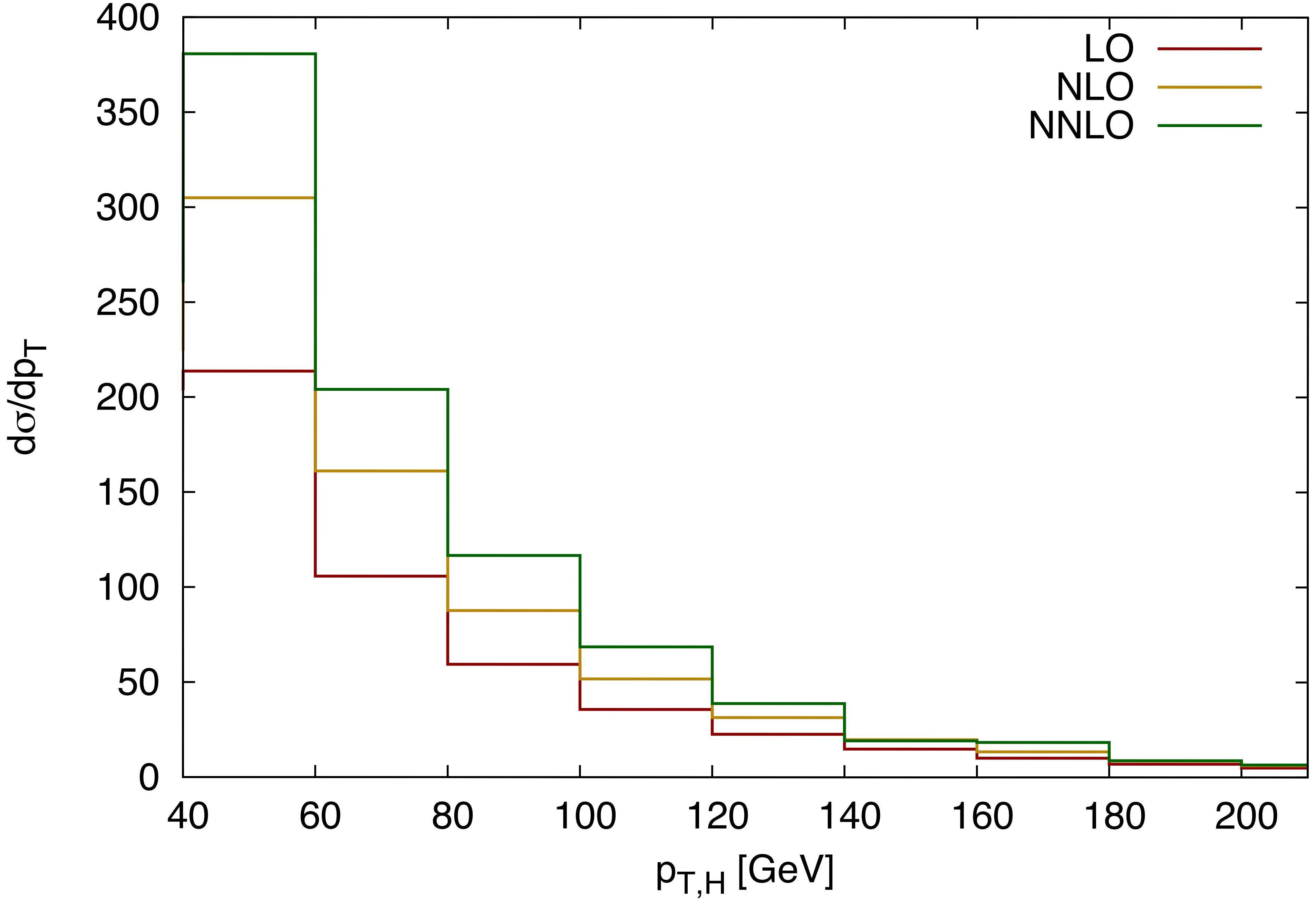

Numerical results

Numerics: gg+qg channels at NNLO, qq at NLO; anti-k_T jets with R=0.5; NNPDF 2.3; $\mu=m_h$

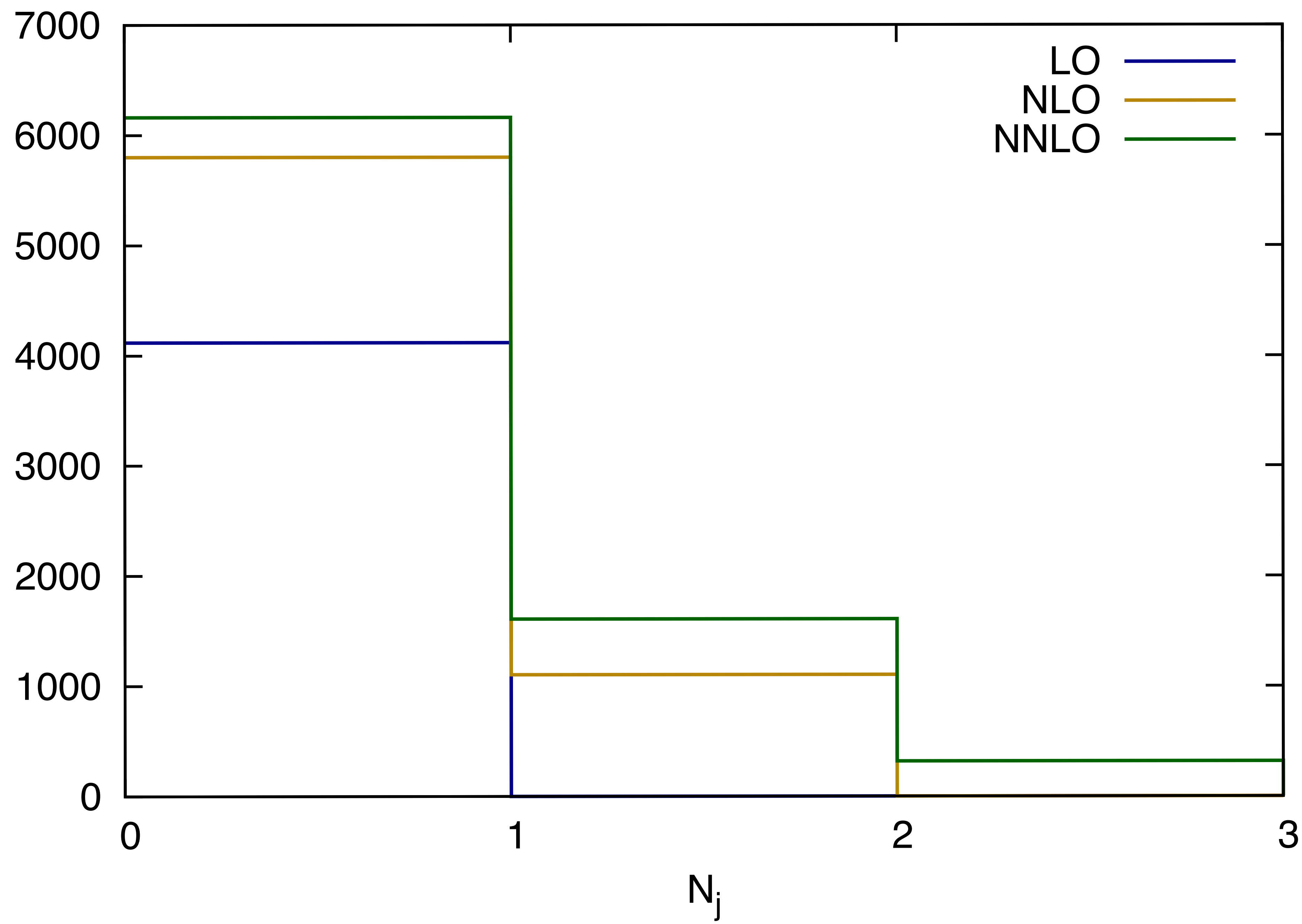

Conclusions

- Great progress in our understanding of H+jet in the past few years, both with fixed-order and resummation
- Significant reduction of theory errors plaguing experimental analyses
- Stay tuned for more results